

SMOOTH-ARM SPIRAL GALAXIES: THEIR PROPERTIES AND  
SIGNIFICANCE TO CLUSTER-GALAXY EVOLUTION

by

Mary Susan Wilkerson

---

A Dissertation Submitted to the Faculty of the

DEPARTMENT OF ASTRONOMY

In Partial Fulfillment of the Requirements  
For the Degree of

DOCTOR OF PHILOSOPHY

In the Graduate College

THE UNIVERSITY OF ARIZONA

1 9 7 9

## INFORMATION TO USERS

This was produced from a copy of a document sent to us for microfilming. While the most advanced technological means to photograph and reproduce this document have been used, the quality is heavily dependent upon the quality of the material submitted.

The following explanation of techniques is provided to help you understand markings or notations which may appear on this reproduction.

1. The sign or "target" for pages apparently lacking from the document photographed is "Missing Page(s)". If it was possible to obtain the missing page(s) or section, they are spliced into the film along with adjacent pages. This may have necessitated cutting through an image and duplicating adjacent pages to assure you of complete continuity.
2. When an image on the film is obliterated with a round black mark it is an indication that the film inspector noticed either blurred copy because of movement during exposure, or duplicate copy. Unless we meant to delete copyrighted materials that should not have been filmed, you will find a good image of the page in the adjacent frame.
3. When a map, drawing or chart, etc., is part of the material being photographed the photographer has followed a definite method in "sectioning" the material. It is customary to begin filming at the upper left hand corner of a large sheet and to continue from left to right in equal sections with small overlaps. If necessary, sectioning is continued again—beginning below the first row and continuing on until complete.
4. For any illustrations that cannot be reproduced satisfactorily by xerography, photographic prints can be purchased at additional cost and tipped into your xerographic copy. Requests can be made to our Dissertations Customer Services Department.
5. Some pages in any document may have indistinct print. In all cases we have filmed the best available copy.

University  
Microfilms  
International

300 N. ZEEB ROAD, ANN ARBOR, MI 48106  
18 BEDFORD ROW, LONDON WC1R 4EJ, ENGLAND

8008059

WILKERSON, MARY SUSAN

SMOOTH-ARM SPIRAL GALAXIES: THEIR PROPERTIES AND  
SIGNIFICANCE TO CLUSTER-GALAXY EVOLUTION

*The University of Arizona*

PH.D.

1979

University

Microfilms

International

300 N. Zeeb Road, Ann Arbor, MI 48106

18 Bedford Row, London WC1R 4EJ, England

PLEASE NOTE:

In all cases this material has been filmed in the best possible way from the available copy. Problems encountered with this document have been identified here with a check mark ☒.

1. Glossy photographs ☒
2. Colored illustrations \_\_\_\_\_
3. Photographs with dark background \_\_\_\_\_
4. Illustrations are poor copy \_\_\_\_\_
5. Print shows through as there is text on both sides of page \_\_\_\_\_
6. Indistinct, broken or small print on several pages \_\_\_\_\_ throughout  
\_\_\_\_\_
7. Tightly bound copy with print lost in spine \_\_\_\_\_
8. Computer printout pages with indistinct print \_\_\_\_\_
9. Page(s) \_\_\_\_\_ lacking when material received, and not available  
from school or author \_\_\_\_\_
10. Page(s) \_\_\_\_\_ seem to be missing in numbering only as text  
follows \_\_\_\_\_
11. Poor carbon copy \_\_\_\_\_
12. Not original copy, several pages with blurred type \_\_\_\_\_
13. Appendix pages are poor copy \_\_\_\_\_
14. Original copy with light type \_\_\_\_\_
15. Curling and wrinkled pages \_\_\_\_\_
16. Other \_\_\_\_\_



SMOOTH-ARM SPIRAL GALAXIES: THEIR PROPERTIES AND  
SIGNIFICANCE TO CLUSTER-GALAXY EVOLUTION

by

Mary Susan Wilkerson

---

A Dissertation Submitted to the Faculty of the

DEPARTMENT OF ASTRONOMY

In Partial Fulfillment of the Requirements  
For the Degree of

DOCTOR OF PHILOSOPHY

In the Graduate College

THE UNIVERSITY OF ARIZONA

1 9 7 9

THE UNIVERSITY OF ARIZONA  
GRADUATE COLLEGE

I hereby recommend that this dissertation prepared under my direction  
by Mary Susan Wilkerson  
entitled Smooth-Arm Spiral Galaxies: Their Properties  
and Significance to Cluster-Galaxy Evolution  
be accepted as fulfilling the dissertation requirement for the Degree  
of Doctor of Philosophy.

Stephen E. Strom  
Dissertation Director

10/30/79  
Date

As members of the Final Examination Committee, we certify that we have  
read this dissertation and agree that it may be presented for final  
defense.

J R Angel  
T H Swihart  
David Dedera  
W G Tipton

31/10/79  
Date  
10/31/79  
Date  
10/31/79  
Date  
Nov 1, 1979  
Date  
\_\_\_\_\_  
Date

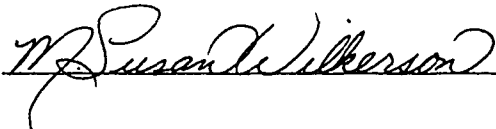
Final approval and acceptance of this dissertation is contingent on the  
candidate's adequate performance and defense thereof at the final oral  
examination.

STATEMENT BY AUTHOR

This dissertation has been submitted in partial fulfillment of requirements for an advanced degree at The University of Arizona and is deposited in the University Library to be made available to borrowers under rules of the Library.

Brief quotations from this dissertation are allowable without special permission, provided that accurate acknowledgment of source is made. Requests for permission for extended quotation from or reproduction of this manuscript in whole or in part may be granted by the head of the major department or the Dean of the Graduate College when in his judgment the proposed use of the material is in the interests of scholarship. In all other instances, however, permission must be obtained from the author.

SIGNED:

\_\_\_\_\_



## ACKNOWLEDGMENTS

Acknowledgment writing is like packing for a trip -- no matter how many times you review what you are taking, you always forget something (or someone). Conversely, you simply can't take everything you think you might need (or thank everyone you should have thanked). With that apology, onward . . .

My sincerest thanks go to Steve and Karen Strom; for without their ever-available help, patience and patronage, this dissertation would never have been written. Bill Romanishin provided immense moral and scientific support, and interesting Friday evenings. Pete Worden will climb onto the smallest limb to help his friends, and this he has done for me more than once. I thank Duane Carbon for stimulating discussions and for an understanding of hunger. I would like to acknowledge Steve Grandi for no particular reason except that he is a good friend and he cited me in his thesis acknowledgments. My first two years in graduate astronomy Peter Strittmatter provided guidance not only toward scientific achievement but also toward scientific maturity. I thank Geoff Burbidge for a graceful transition.

The scientific staffs of Kitt Peak National Observatory, Steward Observatory and Sacramento Peak Observatory have, with few exceptions, always been helpful and considerate. I thank KPNO in particular for use of their data-reduction facilities. Myrna Cook, Pete Gural and the KPNO photolab provided the technically lovely figures in this dissertation. Arecibo Observatory and Hale Observatories provided observing time, data from which are included herein.

I would like to thank Aleta Ara, Taras, Eduín Moonstruck, Wotan du Roc, Eléana, George of Port Kar, Peregryne Tal Elan of Non, James Darkstar, Steffan the Well-Learned, and members of the Society for Creative Anachronism for an alternate reality.

Finally, but foremost, I wish to thank my parents; for without their confidence, understanding and love I would never have begun, much less finished, my Ph. D.

I will close these acknowledgments with the inspired words of Bob Dylan as motivation for those yet in the mill:

Twenty years of schoolin' and they put you on  
the day shift.  
Look out kid;  
They keep it all hid.

## TABLE OF CONTENTS

	Page
LIST OF TABLES . . . . .	vii
LIST OF ILLUSTRATIONS . . . . .	viii
ABSTRACT . . . . .	ix
1. INTRODUCTION . . . . .	1
2. OBSERVATIONS . . . . .	18
Optical Observations . . . . .	18
Identifying Smooth-arm Spirals: The	
Cluster Plate Material . . . . .	18
Photographic Photometry . . . . .	25
Photoelectric Photometry and Calibra-	
tion of Photographic Photometry . . . .	30
Morphological Typing . . . . .	39
Image-tube Direct Photography . . . . .	40
Spectroscopy . . . . .	44
21-cm Observations . . . . .	44
3. RESULTS . . . . .	52
The Photographic Photometry . . . . .	52
Annular-aperture Photometry . . . . .	52
"Azimuthal" Photometry . . . . .	62
Photometry Comparisons and Error	
Trends . . . . .	63
Color Comparisons between Smoothies	
and Normal Galaxies . . . . .	67
Arm and Disk Surface Photometry . . . . .	72
Comparison between Morphological	
Classifications . . . . .	80
Disk-to-bulge Ratios . . . . .	81
Other Optical Observations . . . . .	85
The Search for Smooth-arm Spirals in	
the Field . . . . .	85
Spectroscopic Observations . . . . .	87
Neutral Hydrogen Results . . . . .	88

TABLE OF CONTENTS--Continued

	Page
4. DISCUSSION . . . . .	88
REFERENCES . . . . .	106

## LIST OF TABLES

Table	Page
1. Photographic Plate Data . . . . .	21
2. List of Smooth-arm Spiral Galaxies . . . . .	22
3. Photoelectric Photometry . . . . .	31
4. Filter Combinations for Photoelectric Observations . . . . .	34
5. Photographic Record of Candidate Smooth- arm Spirals in the Field or in Small Associations . . . . .	43
6. Optical Spectroscopic Data . . . . .	45
7. Results of Neutral Hydrogen Observations of Five Smooth-arm Spirals and Four Non-smooth Cluster Galaxies . . . . .	49
8. Annular- and Circular-aperture Photographic Photometry . . . . .	53
9. Comparisons between Galaxy Magnitudes in Three Systems . . . . .	64
10. Numerical Value Assignments for Morphological Types . . . . .	71
11. Arm-strength Rankings . . . . .	79
12. Disk-to-bulge Ratios for Five Smooth-arm Spirals . . . . .	84
13. Total Galaxy Counts and Spi:Smo Ratio . . . . .	100
14. Limiting Absolute Magnitudes for Galaxies Considered in Cluster Galaxy Counts . . . . .	103



# LIST OF ILLUSTRATIONS

Figure		Page
1.	The Thirty-three Smooth-arm Spiral Galaxies Studied in this Work . . . . .	9
2.	Comparisons between Photoelectric Magnitudes and Photographic Raw Magnitudes for Three Typical Clusters . . . . .	36
3.	(U-B) vs. (U-R) and (B-R) vs. (U-R) Color-color Plots . . . . .	38
4.	Color vs. Morphological Type for Non- smooth-arm Cluster Galaxies and for Smooth-arm Spirals . . . . .	68
5.	Values of $(U-R)_{\text{disk}} - (U-R)_{\text{arms}}$ for Fourteen Smooth-arm Spirals . . . . .	73
6.	Plot of Color vs. $U_{\text{max}}$ Arm Amplitude for Eleven Smooth-arm Spirals . . . . .	76
7.	21-cm Spectrum of UGC 1350 . . . . .	89
8.	21-cm Spectrum of UGC 1344 . . . . .	90
9.	21-cm Spectrum Toward NGC 495 . . . . .	91
10.	X-ray Luminosity and Abell Richness Class vs. $\text{Spi:Smo}$ Ratio for Five Abell Clusters Containing Smooth-arm Spirals . .	99

## ABSTRACT

We have examined a number of galaxies with optical appearances between those of normal, actively-star-forming spirals and S0 galaxies. These so-called smooth-arm spiral galaxies exhibit spiral arms without any of the spiral tracers -- H II regions, O-B star associations, dust -- indicative of current star formation.

Tests were made to find if, perhaps, these smooth-arm spirals could have, at one time, been normal, actively-star-forming spirals whose gas had been somehow removed; and that are currently transforming into S0 galaxies. This scenario proceeds as (1) removal of gas, (2) gradual dying of disk density wave, (3) emergence of S0 galaxy. If the dominant method of gas removal is ram-pressure stripping by a hot, intracluster medium, then smooth-arm spirals should occur primarily in x-ray clusters.

The major findings of this dissertation are as follows:

1. Smooth-arm spirals are redder than normal spirals of the same morphological type. Most smooth-arm spirals cannot be distinguished by color from S0 galaxies.

2. A weak trend exists for smooth-arm spirals with stronger arms to be bluer than those with weaker arms; thus implying that the interval since gas removal has been shorter for the galaxies with stronger arms.

3. Smooth-arm spirals are deficient in neutral hydrogen -- sometimes by an order of magnitude or, possibly, more.

4. A correlation exists between the x-ray luminosity of a cluster and the ratio of normal spirals to smooth-arm spirals within that cluster, with the more x-ray luminous clusters having a lower ratio.

5. Smooth-arm spirals exhibit a wide range of disk-to-bulge ratios.

6. There seems to be a much lower incidence of the smooth-arm spiral type in regions of low galaxy density than in galaxy clusters.

These results are supportive of the hypothesis that smooth-arm spirals were once actively-star-forming spiral galaxies now in transition to S0s.

## CHAPTER 1

### INTRODUCTION

Classical galaxian morphology as proposed by Edwin Hubble and refined by Allan Sandage (Hubble 1926, 1936; Sandage 1961) distinguishes four basic types.

The first type is the elliptical galaxies. These galaxies have a smooth stellar distribution, negligible cold interstellar gas (Knapp, Kerr and Williams 1978), luminosities typically  $M_V = -20$  to  $-24.5$  (van den Bergh, in press), and are rather red, with (U-R) colors typically 2.2 to 2.8 magnitudes (Biermann and Tinsley 1975). The redness implies that the stellar population is old, for had stars formed recently with any kind of normal initial mass function then there would be hot, massive, luminous, blue stars which would contribute significantly to the integrated galaxy colors. Colors of normal ellipticals do not indicate the presence of significant numbers of such stars. Also elliptical galaxies lack clumpy regions associated with star formation, such as O-B star associations, H II regions, or (in most cases) dust.

Morphologically, the next group is the S0 galaxies. These galaxies have both a spherical, or bulge, component

and a flattened disk component. Recent evidence indicates S0s also may have an extended thick disk distribution (Burstein, in press, Paper III). The stellar distributions also are smooth. S0s show more structure than ellipticals, frequently exhibiting bars, rings, partial rings, etc. Dust patches are occasionally seen in S0s, mostly on or near the nuclear bulge (Sandage 1961). The luminosity function of S0s peaks at fainter magnitudes than does that for ellipticals, and extends from  $M_V = -18.5$  to  $-24$  (van den Bergh, in press). Neutral hydrogen detections are relatively rare (Knapp et al. 1977). Although some S0 galaxies have a higher mass in interstellar gas than do ellipticals, most S0s seem to be relatively gas poor (Krumm and Salpeter 1979). S0 galaxies can have integrated colors as red as ellipticals; they extend further blueward by up to 0.4 magnitudes<sup>1</sup> (Biermann and Tinsley 1975).

The third class consists of the spiral galaxies. The spirals have a bulge component, a disk component, spiral-arm structure in the disk, and a halo. For the most part, the bulge, disk and halo consist of older stars while the spiral arms are traced primarily by younger stars. The arms are the sites of current star formation. In the arms of most spirals can be seen hot, blue O-B star associations,

---

<sup>1</sup>Unless noted otherwise, all colors given in this paper will be in magnitudes of (U-R).

H II regions, and dust -- all evidence for active star formation. These regions are referred to as spiral tracers as they are the most prominent luminous matter in the spiral arms. They give the arms a patchy or clumpy appearance. In the density-wave theory of spiral structure the arms are viewed as a self-sustaining density pattern in the disk. As the disk gas is accelerated in the vicinity of the density enhancement, the gas is compressed sufficiently to initiate star formation (Wielen 1974; Toomre 1977). Among the newly formed stars are hot, massive, highly-luminous stars that evolve quickly into lower-luminosity forms (white dwarfs, pulsars, black holes) before the young stars drift beyond the density wave crest. Density waves reach amplitudes as high as 30%, with 10-15% being a typical value for the density enhancement in the underlying disk population of stars (Schweizer 1976; Jensen 1977). Surface photometry of spirals confirms the morphological evidence that spiral arms have young stars. The (U-R) arm colors of Sb's and Sc's are typically 0.8 to 1.3 magnitudes, and the underlying disk colors are 1.6 to 2.2 magnitudes (Schweizer 1976). Spiral luminosities have a wide range, from luminosities equal to or slightly greater than the brightest S0s to very faint luminosities around  $M_V = -17$  (Dressler, in press; Strom, in press).

The last Hubble classification is the irregular galaxies. Their properties will be considered only very briefly here as irregulars are not central to this dissertation. Irregulars, as their name implies, have no set structure and no nuclear bulge, although generally a disk is seen. They tend to be quite blue, have many patchy regions of active star formation, and have lower luminosities than the earlier galaxies.

Hubble (1926) originally considered his morphological sequence to be an evolutionary one as well, with irregulars and Sc's evolving through the intermediate types to ellipticals. The idea of one morphological type transmuting into another has periodically gained and lost favor.

Traditionally S0s have been considered to represent a transition stage between spirals and ellipticals. Much attention has been dedicated in the past few years to the possibility that S0s are the evolutionary descendants of spirals. In this scenario S0 galaxies could represent one or more of the following:

1. systems with little disk gas remaining after formation and in which star formation consequently ceased soon thereafter,
2. former spiral galaxies that have exhausted their disk gas in normal evolutionary processes, or

3. former spirals in which disk gas has been somehow removed.

Several recent studies have focused on the last possibility -- specifically that S0s may be spirals that have been stripped of their gas (e.g. Spitzer and Baade 1951; Gunn and Gott 1972; Lea and de Young 1976; Gisler 1979). Spitzer and Baade (1951) considered stripping via galaxy collisions. The Spitzer-Baade hypothesis has lost favor; the collisions would occur primarily in the dense cluster cores and stripping would result for collisions between two galaxies with approximately equal gas masses. Collisions between a galaxy with gas and one already stripped would have little effect on the gas content of the gas-bearing system. Thus there should be more galaxies with gas even in dense-cluster cores than are observed.

In 1972, Gunn and Gott proposed that spiral galaxies in clusters could be stripped of their gas via ram pressure when a galaxy passed through a hot, dense intra-cluster medium. Observational indications of stripping have been examined by Melnick and Sargent (1977), who found that in clusters known to be x-ray sources, and therefore suspected of having hot intracluster media, the ratio of spirals to S0s increases with increasing radius from near zero in the cluster cores. The intracluster gas density also decreases with increasing cluster radius. They found



an inverse correlation between the fraction of galaxies that are spirals and the intensity of the x-ray emission. Dressler (in press) found not only a correlation between the spiral fraction and distance from the cluster center, but also between the spiral fraction and the local galaxy density.

Another possible indication of stripping is shown in studies by Butcher and Oemler (1978a, 1978b). Nearby centrally condensed clusters contain mostly red galaxies and are spiral poor, whereas two centrally-condensed clusters at redshifts near  $z = 0.4$  have many blue galaxies with colors indicative of spiral richness. Between one-third and one half of the galaxies in these two clusters have the colors of present-day spirals. Butcher and Oemler suggest that most of the actively star-forming galaxies have been stripped in the nearby clusters, whereas stripping is incomplete in the more distant clusters.

Recently Forman et al. (in press) have observed with the Einstein X-ray Observatory what they believe to be a galaxy, M 86, caught in the act of being stripped by the intracluster medium in Virgo. If so, this observation would represent the first direct evidence for gas being swept from galaxies.

These above data offer indirect support of the hypothesis that S0s in rich clusters are stripped spirals.

If this transmutation indeed takes place, then what must transition objects look like, and what would be their properties? What lies between a recently star-forming spiral whose gas has been removed and an S0 galaxy, and can we identify it?

A possible scenario for the evolutionary transition of a stripped spiral is

1. loss of population-I tracers such as dust, H II regions, O-B star associations,
2. weakening of the disk density wave, and
3. emergence of a classic S0 galaxy.

The above scenario implies that some cluster galaxies should have the appearance of spiral galaxies -- that is, have spiral arms -- but without the clumpiness due to population-I tracers usually associated with spiral arms. Such galaxies are indeed seen. van den Bergh (1976) has identified a class of galaxies which he calls anemic spirals. He states in the abstract of his 1976 paper that "a sequence of 'anemic spirals,' which occur most frequently in rich clusters, is found to have characteristics that are intermediate between those of vigorous gas-rich normal spirals and gas-poor systems of type S0."

Even more extreme cases of "anemia" have been identified, wherein there is no indication of star formation (Strom, Jensen and Strom 1976; Wilkerson, Strom and

Strom 1977). These galaxies, the topic of this dissertation, shall be called smooth-arm spiral galaxies or "smoothies." The smooth-arm spirals studied in the present work are shown in Figure 1.

What would be the observational consequences if smooth-arm spirals are indeed gas-depleted/stripped spirals in transition to S0s? Let us take the above hypothesis one step at a time.

Most obviously, a spiral galaxy that has had its interstellar gas somehow removed or depleted should have a low neutral-hydrogen content. Depending upon the efficiency of the initial removal, the rate of gas replenishment from stars, and the presence and efficiency of continuing gas sweeping or depletion (such as further traversal of an intracluster medium or onset of galactic winds capable of cleaning the galaxy [Gisler 1979]), we should see H I masses anywhere from slightly subnormal for the morphological type to no H I detection at all, with the upper limits substantially below average.

If this gas-poor spiral cannot replenish its interstellar medium sufficiently to recommence star formation, then after a few  $\times 10^7$  years the galaxy will be quite measurably redder than the progenitor galaxy. Thus a smooth-arm spiral should be too red for its morphological type, assuming that the smoothy stage lasts longer than  $10^7$  years.

Figure 1. The Thirty-three Smooth-arm Spiral Galaxies Studied in this Work. -- Galaxy names, cluster memberships and scale are indicated.

- a. Galaxies in G383.
- b. Galaxies in Pisces.
- c. Galaxies in Abell 262.
- d. Galaxies in Perseus.
- e. Galaxies in Abell 1228.
- f. Galaxies in Abell 1367.
- g. Galaxies in Abell 2199.

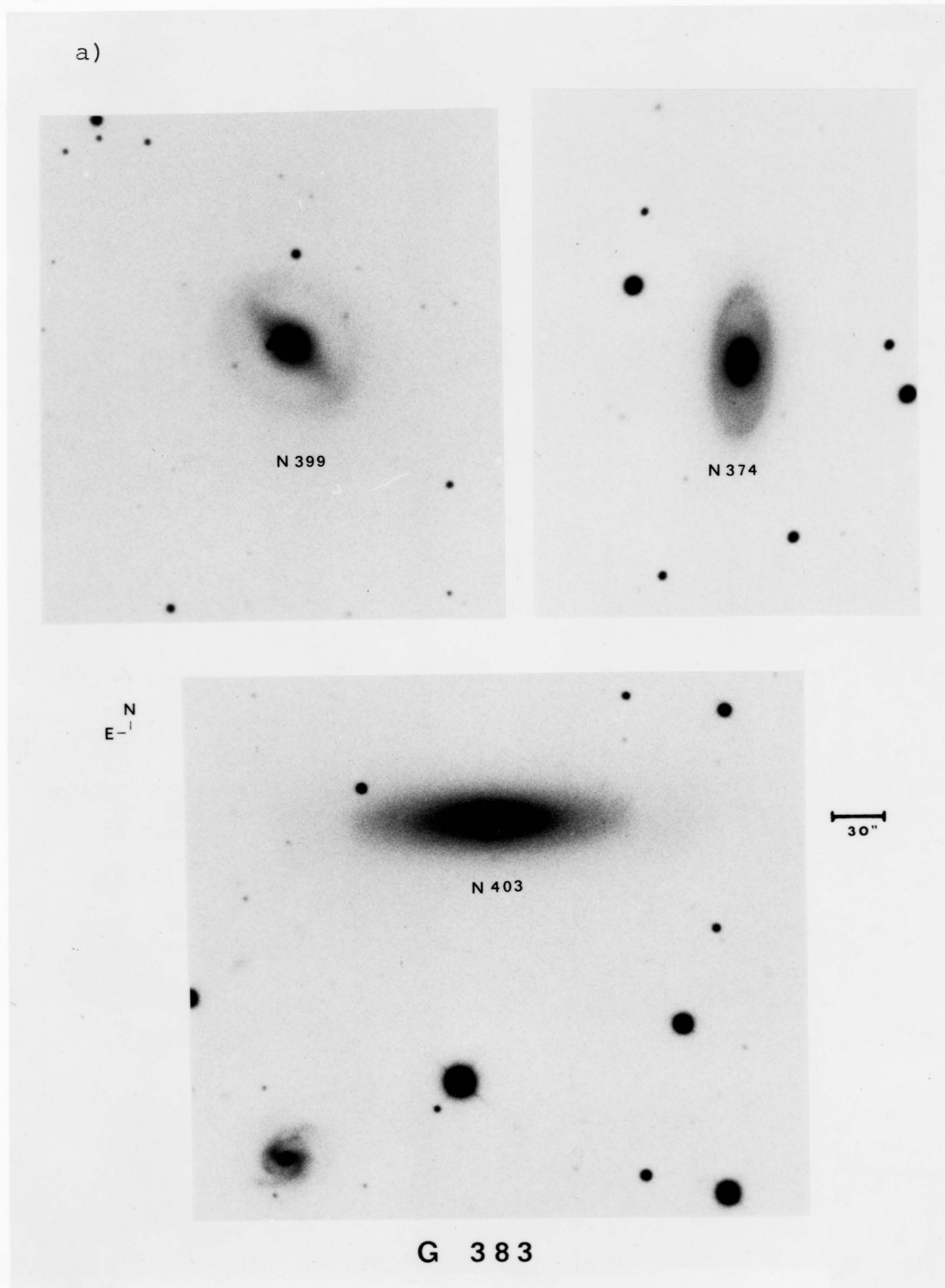


Figure 1. Smooth-arm Spiral Galaxies.

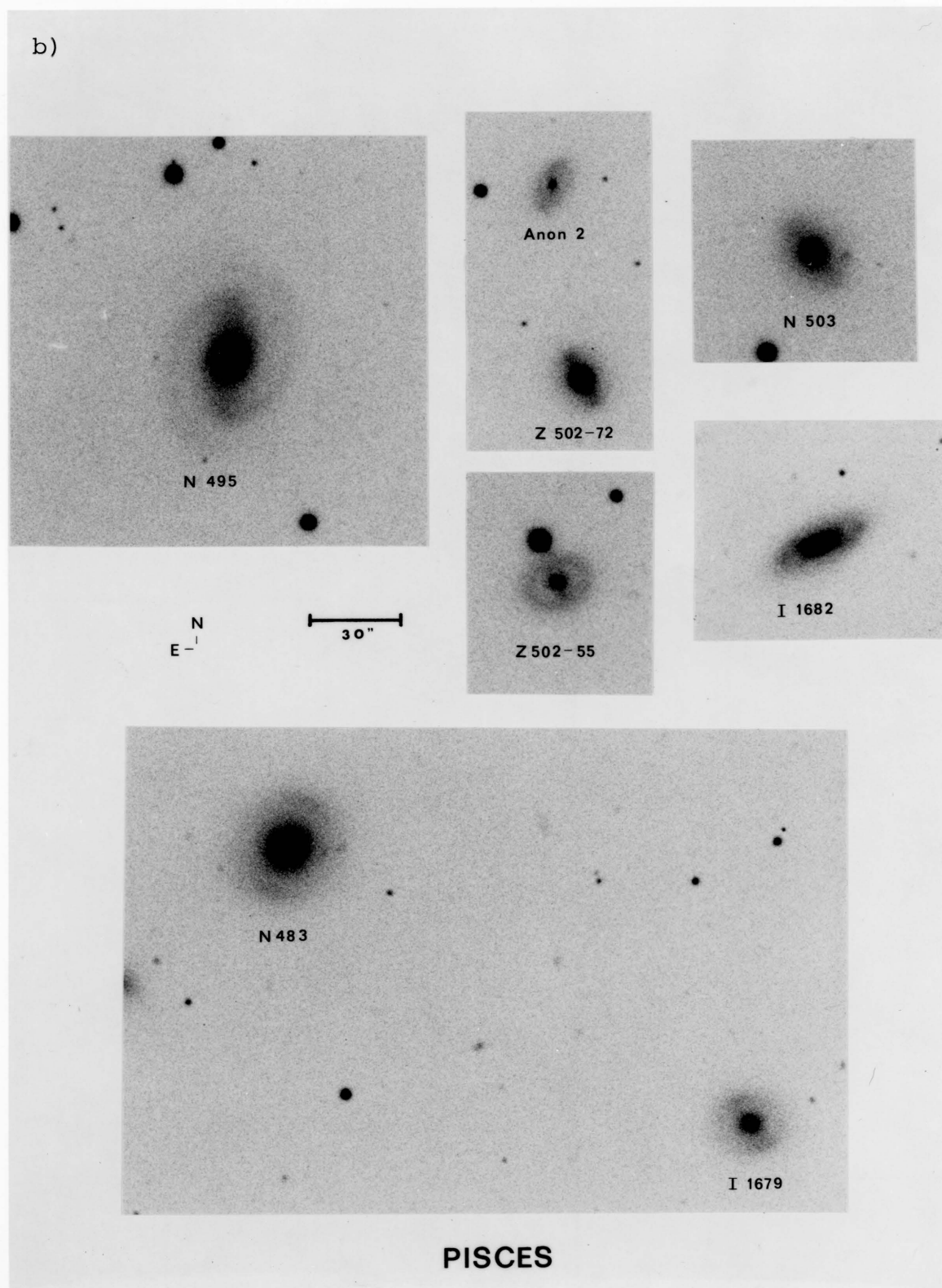


Figure 1. Continued. -- Smooth-arm Spiral Galaxies.

c)

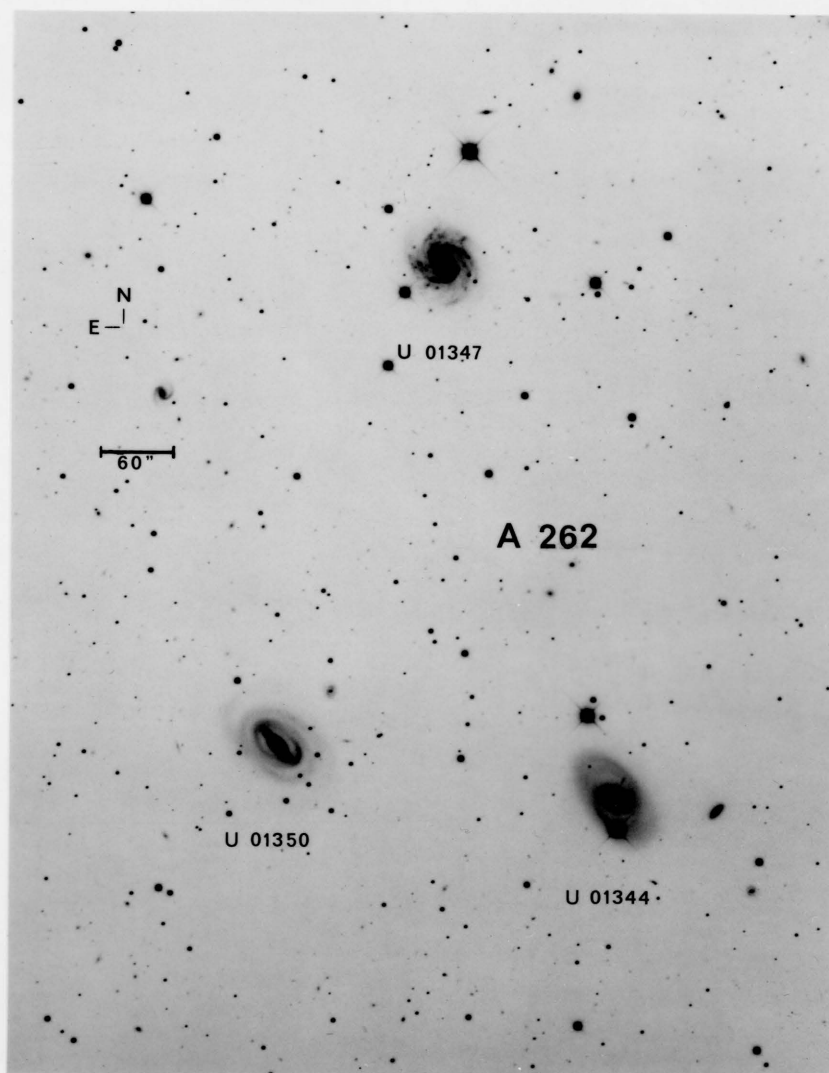


Figure 1. Continued. -- Smooth-arm Spiral Galaxies.

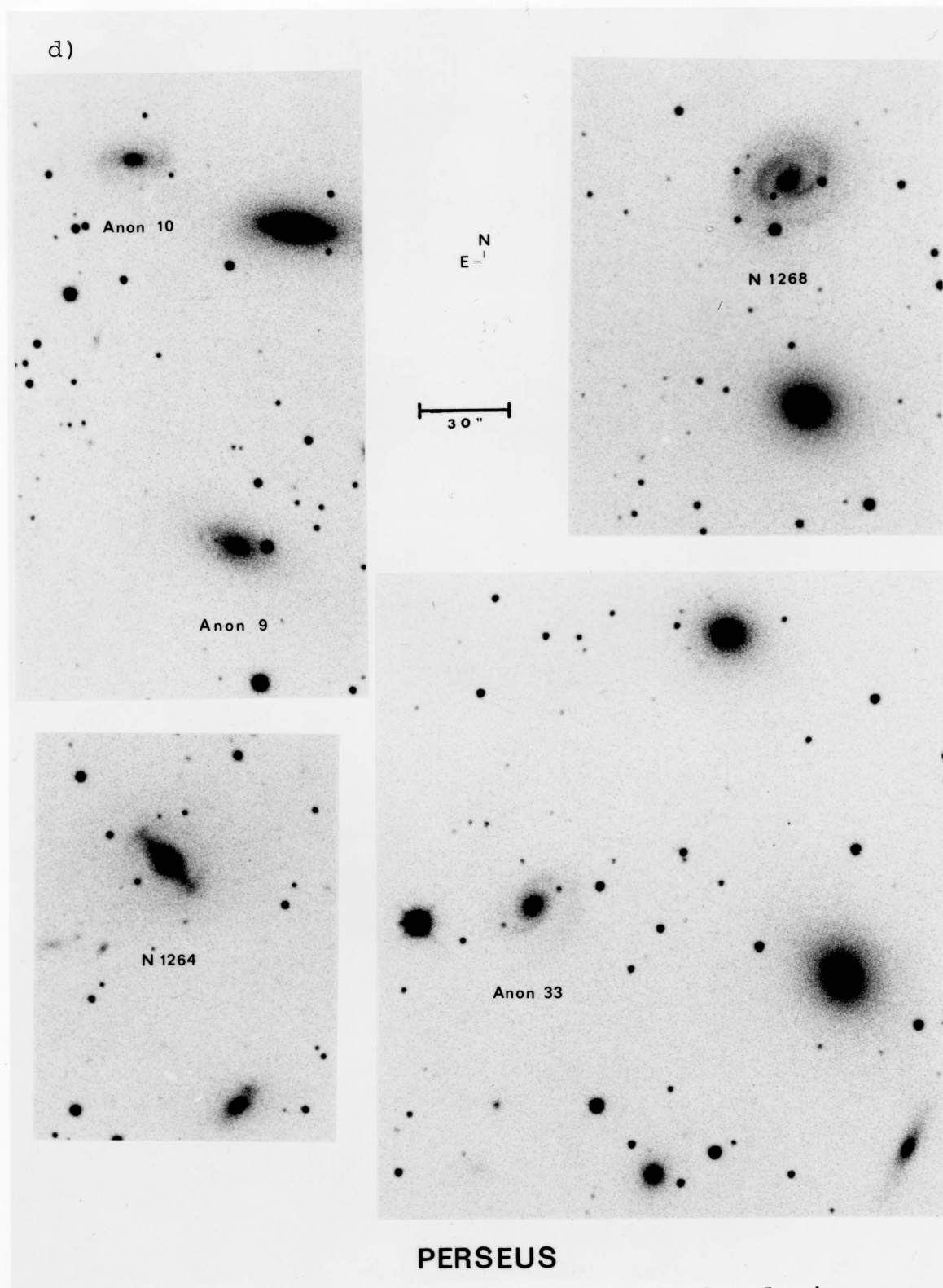


Figure 1. Continued. -- Smooth-arm Spiral Galaxies.



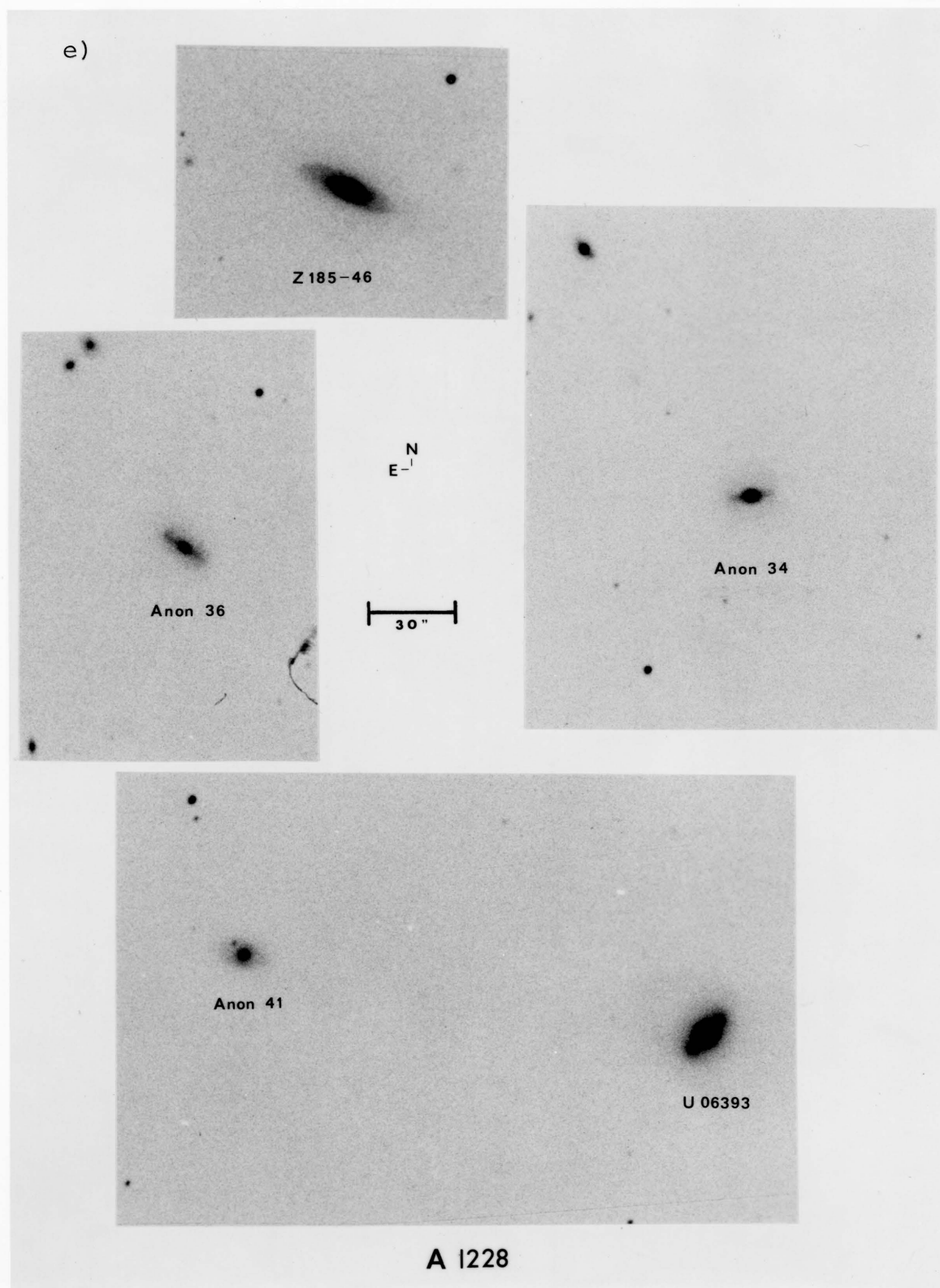


Figure 1. Continued. -- Smooth-arm Spiral Galaxies.

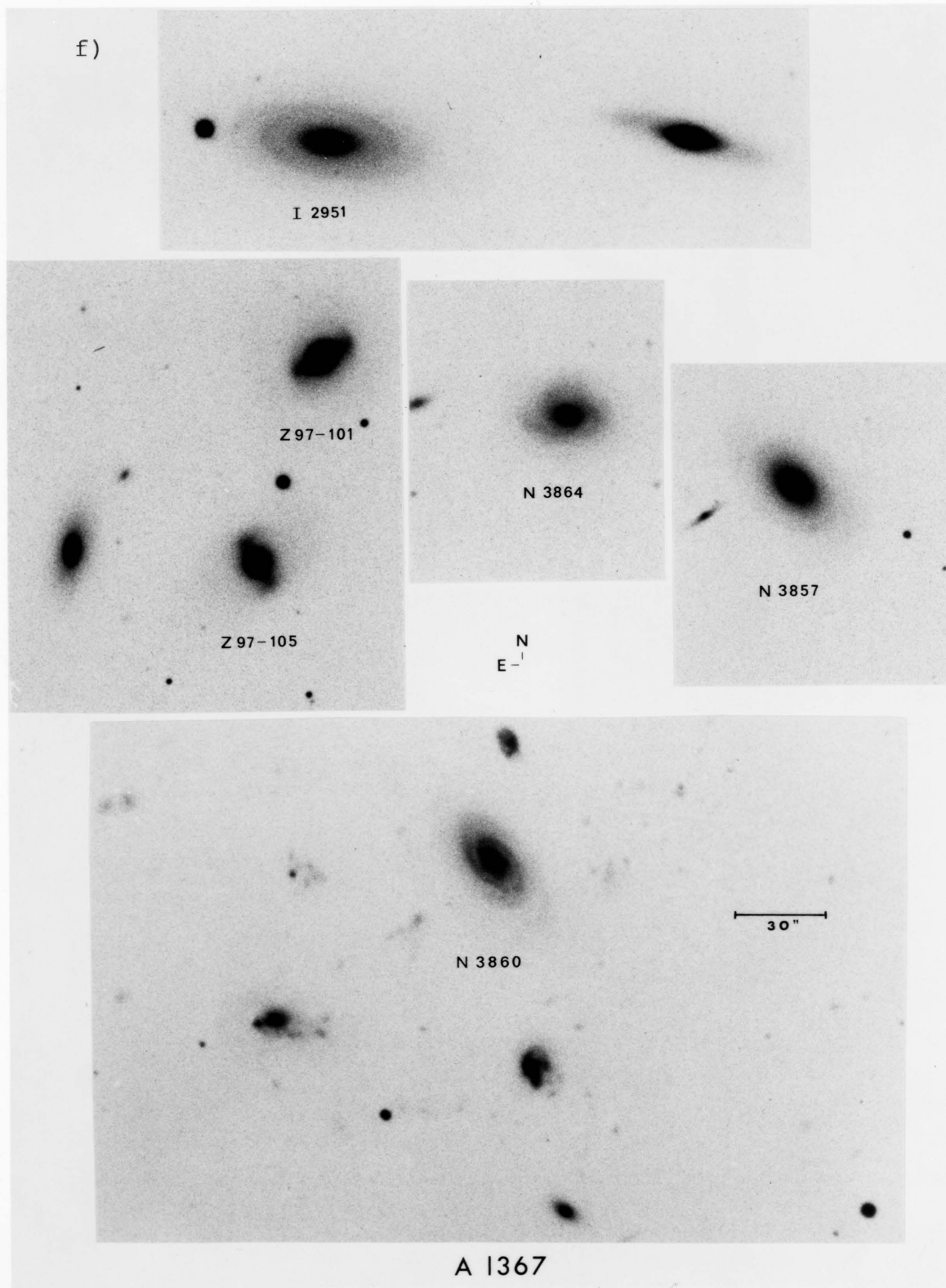
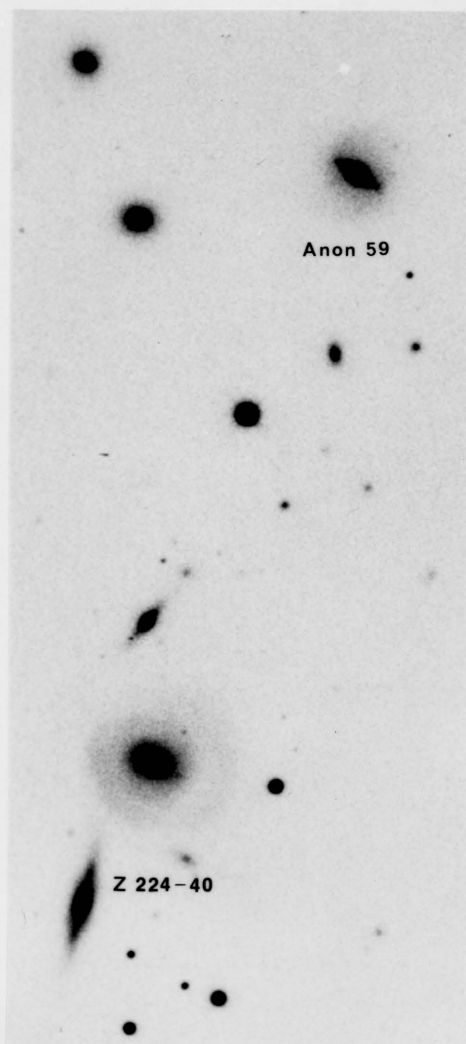
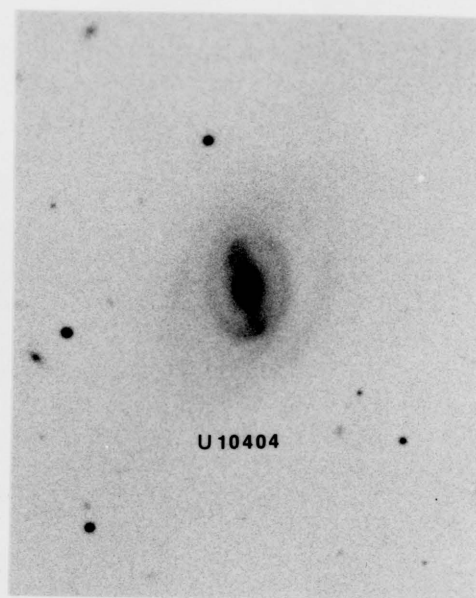
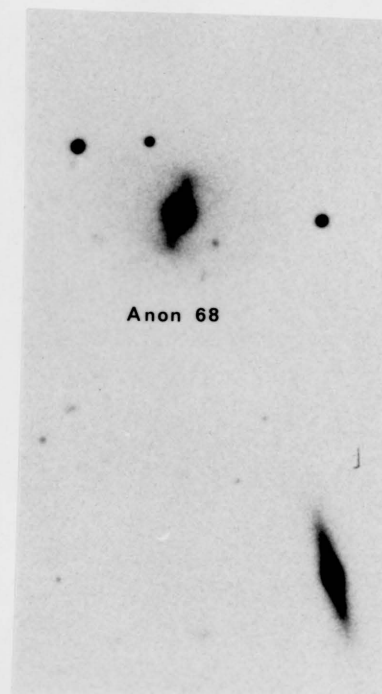


Figure 1. Continued. -- Smooth-arm Spiral Galaxies.

g)

N  
E

30"



A 2199

Figure 1. Continued. -- Smooth-arm Spiral Galaxies.

It will require  $\sim 2 \times 10^7$  years for O-B associations to die out; thus a gas-free spiral would not be recognized as a smooth-arm spiral for the first 20 million years or so after the gas removal or depletion.

What if our hypothetical gasless spiral evolves into an S0 galaxy? We might expect a correlation between the arm strength and the color. As the evolution toward S0 proceeds, the disk density wave will, by requirement, decrease in strength; at the same time the color will grow progressively redder as the time since the last star formation events increases. Of course such a correlation might be partially obscured by such factors as initial galaxian colors and morphological type, and definition of arm "strength."

If smoothies represent primarily normal spirals that have been stripped by a hot, intracluster medium, then we would anticipate a much lower rate of smooth-arm spirals in the field. Those smoothies in the field would be systems in which gas was removed by processes intrinsic to the galaxy itself -- astration and galactic winds, for example. Also we might expect a relation between the cluster x-ray luminosity and the ratio of normal spirals to smoothies; if the x-ray luminosity is higher, then, at constant temperature, the intracluster medium is denser, and more spirals can be stripped to produce smoothies. The spiral-to-smoothy

ratio will depend primarily upon the time scale during which a stripped spiral can be recognized as a smoothy rather than as an S0.

These above speculations shall be taken up in the following chapters. We will present the observations made and data obtained in Chapter 2. Chapter 3 contains the results of these data. Chapter 4 is devoted to discussion on the implications of the results given in Chapter 3.

## CHAPTER 2

### OBSERVATIONS

Photographic surface photometry, photoelectric photometry, direct and image-tube direct photography, spectroscopy and radio spectral-line observations were employed in the study of smooth-arm spirals. The optical observations are used to find integrated galaxian colors, and colors separately of the arms and disks of smooth-arm spirals. These observations are intended to test the hypothesis that smoothies indeed represent systems in which star formation has effectively ceased. Also described is a limited search for "field smoothies." The descriptions of optical observations are followed by a discussion of a 21-cm search for neutral hydrogen in these galaxies. These data were used to assess the degree of gas-depletion in these systems.

#### Optical Observations

Identifying Smooth-arm Spirals:  
The Cluster Plate Material

Photographic plates of several fairly nearby clusters of galaxies were examined visually to find smooth-arm spirals. The plates all were obtained at the prime focus of the Kitt Peak National Observatory (KPNO) Mayall 4-meter



telescope. Deep plates with passbands corresponding to the standard U and R photometric bands (Kron and Smith 1951; Johnson and Morgan 1951; Johnson 1963) were examined. To be classified as a smooth-arm spiral, a galaxy had to appear entirely smooth on all plates under 8x eyepiece magnification. The smooth-arm spirals thus identified were further sorted into good candidates (M) and fair candidates (m). A smoothy would generally receive a fair classification for one or more of the following deficiencies:

1. too small or too faint to determine with certainty whether it is truly smooth or merely anemic,
2. arms of such low strength that it is difficult to decide reliably on their existence,
3. appearance of very slight clumpiness under higher magnification or with digital processing.

In addition, the material for some clusters could not be discussed because the cluster distances were too great to distinguish smoothies from anemics. Other candidate smoothies, such as NGC 4596 and NGC 4608 in Virgo, regretfully must await future studies due to incomplete plate coverage (specifically, deep U plates were not available).

The above identification process and subsequent photographic photometry were conducted using prime-focus direct plates exposed at the KPNO Mayall 4-meter telescope. For each cluster a deep U plate (IIIa-J and UG2) and an R

plate (IIIa-F or 098 and RG610) were used. Table 1 presents a summary of the photographic plate material used in this investigation.

The long (U-R) baseline provides a good discriminant between disk populations and "normal" spiral arms with population-I tracers (Strom, Jensen and Strom 1976). The U photometric band transmits the [OII]  $\lambda 3727$  emission from gaseous nebulae associated with star formation. O and B star fluxes peak in the U band or blueward, thus, if significantly present, dominating the stellar thermal contribution. The contributions from older disk populations are relatively low. Conversely the R band includes light emitted primarily by K-giants and other low-mass stars.

Eighteen nearby clusters with  $z_{\text{cluster}} \lesssim .04$  were searched for smooth-arm spirals. All but two clusters -- Cancer and Abell 586 -- contained smoothies. Some clusters were discarded due to inadequate plate coverage or unfavorable declination ranges. Future investigations of smooth-arm spirals should incorporate such additional clusters. In all, 33 good or fair smooth-arm spirals in 6 clusters of galaxies and one group were included in this study. The clusters are Pisces (sometimes called the NGC 507 cluster), a group centered on NGC 383 (G383), Abell 262, Perseus (Abell 426), Abell 1228, Abell 1367 and Abell 2199 (Abell 1958). Table 2 lists the smooth-arm spirals studied, along



Table 1. Photographic Plate Data.

Plate #	Cluster	Emulsion	Filter	Exposure Length	Date
1812	Perseus	III a-J	UG-2	135 min.	10/29/75
1813	Perseus	098-04	RG-610	40 min.	10/29/75
1841	Pisces	098-04	RG-610	55 min.	12/01/75
1907	A262	III a-J	UG-2	142 min.	1/30/76
2197	G383	III a-F	RG-610	60 min.	12/21/76
2206	G383	III a-J	UG-2	120 min.	12/22/76
2211	A1367	III a-F	RG-610	55 min.	12/22/76
2212	A1367	III a-J	UG-2	120 min.	12/22/76
2216	Pisces	III a-J	UG-2	120 min.	12/23/76
2230	A262	III a-F	RG-610	55 min.	12/24/76
2295	A1228	III a-J	UG-2	110 min.	2/13/77
2296	A1228	III a-F	RG-610	40 min.	2/13/77
2307	A2199	III a-F	RG-610	55 min.	2/14/77
2314	A2199	III a-J	UG-2	110 min.	2/15/77

Table 2. List of Smooth-arm Spiral Galaxies. -- The velocity listed after the cluster name is the cluster mean velocity.

Cluster	Name	Other Names	R.A. (1950)	Dec. (1950)	$V_r$ (km s <sup>-1</sup> )	Source <sup>a</sup>
G383					5261	
	N374	Z501-80 U680	01 04 19.9	+32 31 40	5067	5
	N399	Z501-101 U712	01 06 13.1	+32 22 04	5167	5
	N403	Z501-104 U715	01 06 27.9	+32 29 09	4977	5
Pisces					4437	
	I1679	Z502-48	01 18 55.6	+33 13 56		
	N483	Z502-50 U906	01 19 07.3	+33 15 35		
	I1682	Z502-53 U912	01 19 24.4	+32 59 56		
	Z502-55		01 19 45.2	+32 50 32		
	N495	Z502-58 U920	01 20 06.9	+33 12 38	4114	4
	N503	Z502-65	01 20 39.4	+33 04 17	6177	7
	Anon 2		01 21 09.3	+33 03 10		
	Z502-72		01 21 09.9	+33 04 15		

Table 2.--Continued

Cluster	Name	Other Names	R.A. (1950)	Dec. (1950)	$V_r$ (km s <sup>-1</sup> )	Source <sup>a</sup>
A262					5126	
	U1344	Z522-35	01 49 38.1	+36 15 17	4428	5
	U1350	Z522-42	01 50 00.7	+36 16 00	4975	1
Perseus					5429	
	Anon 9		03 14 11.2	+41 11 34	6561	2
	Anon 10		03 14 14.1	+41 13 44	6077	2
	N1264	U2643	03 14 41.3	+41 20 17	3365	2
	N1268	Z540-93 U2658	03 15 26.8	+41 18 27	3243	2
	Anon 33		03 17 02.5	+41 11 12		
A1228					10313	
	Anon 34		11 17 25.0	+34 24 06		
	Anon 36		11 18 52.5	+34 28 10		
	Z185-46		11 19 21.7	+34 35 20		
	U6393	Z185-50	11 20 12.2	+34 36 56		
	Anon 41		11 20 24.2	+34 37 30		
A1367					6146	
	I2951	Z97-82 U6688	11 40 49.0	+20 01 39	6100	6



Table 2.--Continued

Cluster	Name	Other Names	R.A. (1950)	Dec. (1950)	$V_r$ (km s <sup>-1</sup> )	Source <sup>a</sup>
	Z97-101		11 41 43.4	+20 07 20	6424	1
	Z97-105		11 41 45.2	+20 06 13	5524	1
	N3860	Z97-120 U6718	11 42 13.7	+20 04 21	5461	3
	N3857	Z97-117	11 42 14.8	+19 48 37	5734	1
	N3864	Z97-130	11 42 40.2	+19 40 11	6924	6
A2199					9354	
	U10404	Z224-35	16 26 29.2	+39 55 53	7978	1
	Anon 59		16 26 56.3	+39 37 39		
	Z224-40		16 27 01.4	+39 34 57	9657	1
	Anon 68		16 27 37.0	+39 32 13		

- a. Sources: 1, this study  
 2, Chincarini and Rood (1971)  
 3, Gudehus (1976)  
 4, Humason, Mayall and Sandage (1956)  
 5, Moss and Dickens (1977)  
 6, Tifft (1978)  
 7, Tifft, Hilsman and Corrado (1975)

with their 1950 coordinates, cluster memberships and redshifts (if known).

On each plate a graduated series of 16 calibration spots was exposed on an otherwise unexposed section of the plate. The method for converting photographic density to intensity will be discussed in the next section.

### Photographic Photometry

The photographic plate material was digitized using a Photo Data Systems (PDS) 1010A microdensitometer controlled by a PDP 8/m computer. Selected areas were scanned on each plate using a  $100\text{ }\mu\text{m} \times 100\text{ }\mu\text{m}$  square aperture sampled in  $50\text{ }\mu\text{m}$  steps for all clusters except Abell 262 and Abell 1367. The selected areas in these two clusters were scanned with a  $50\text{ }\mu\text{m} \times 50\text{ }\mu\text{m}$  aperture in  $25\text{ }\mu\text{m}$  steps. The larger pixel size corresponds to a box 1.856 arcseconds on a side, and the smaller to .928 arcsec. All regions scanned at the larger pixel size were either  $512 \times 512$  pixels or  $1024 \times 1024$  pixels; the smaller pixel-size rasters were  $1024 \times 1024$  or  $2048 \times 2048$ . On each plate a small hole was scratched in the emulsion before scanning. Zero density was set to be the density of this region of clear plate. The PDS can then record densities up to a maximum of 5.115. In general only the centers of brighter stars were saturated. Occasionally the nuclei of brighter

galaxies were saturated on the R plate. These saturated regions were always <3 arcsec and usually <1 arcsec.

The calibration spots on each plate were scanned with the same aperture size and spacing as used on the rest of the plate, but the rasters for each spot were only 30 x 30 pixels.

The photographic surface photometry, the density-to-intensity conversions and several other operations, such as determining minor-to-major axis ratios, position angles and galaxy centers were performed on the Interactive Picture Processing System (IPPS) at KPNO (Wells 1975).

The calibration spot rasters were fit to a characteristic curve using a function of the form introduced by Goad (1975). The Goad function is:

$$\log I = P_0 + P_1 Y + P_2 Y^2 + P_3 Y^3 \quad (1)$$

where

$$Y = D + P_4 \log_{10} (1 - 10^{-D}); \quad (2)$$

I is intensity; D is density; and the P's are constants determined by the fit. Saturated spots and bad spots could be deleted from the fit.

The resultant characteristic curve was applied to each pixel on that plate to convert the density rasters to

intensity rasters. The resultant intensity rasters were used for the IPPS reductions throughout this study.

One IPPS routine simulates circular-aperture photometry. The apertures used had diameters of 4", 10", 15", 20", 40" and 60". In addition, galaxies that had photoelectric observations also were measured with the appropriate photoelectric apertures. In order to assess the relation of smoothies to other morphological types, a selection of galaxies of differing morphological types were studied in each cluster.

The circular-aperture photometry also was employed to find colors in annular apertures. This procedure was of great benefit in that such an approach permits a crude separation of bulge and disk light. It is presumed that active star formation takes place in the disk, whereas star formation in the bulge component was completed within  $10^9$  years of the epoch of galaxy formation. The annular apertures selected to aid in bulge subtraction had inner and outer radii of 2" - 5", 5" - 10", 7.5" - 20" and 10" - 30".

For the larger-angular-diameter smooth-arm spirals that were nearly face-on, small (typically 4" diameter) apertures were used to sample galaxian light as a function of radius from the center for both arm and interarm (disk) regions of the galaxies. In such a manner arm and disk brightness and colors could be compared. However, due to

the smaller number of pixels sampled in this procedure the statistical noise both per aperture and per total sampled area is much larger than in the standard aperture photometry.

The galaxies for which 21-cm neutral hydrogen measurements were made required B magnitudes in order to estimate  $m_{\text{HI}}/L_B$  with sufficient accuracy. Magnitudes were obtained internal to the 26.5 magnitude/arcsec<sup>2</sup> isophote in B. Independent measurements were made in U and in R, and converted to the B system using the color-color relations discussed at the end of this section.

Finally, an IPPS routine to sample small circular apertures along a chosen radius vector was employed to "scan" the major axes of some smooth-arm spirals in order to derive bulge and disk parameters from analysis of the major-axis profiles.

In all of the above IPPS photometric procedures, allowances were made for subtracting sky-brightness contributions to the galaxian light. For the aperture photometry an average sky value was determined about a circle centered on the galaxy image. The circle radius is selected by the observer and more than one sky circle can be chosen at different radii to assure a properly chosen sky value. The sky value thus determined is subtracted from the intensity measured within a given aperture to give galaxy minus sky.



For the other photometric procedures a more sophisticated sky-fitting routine was employed. This routine attempts to take into account the density gradient found on 4-m plates. Sky intensities are sampled about a circle centered on the galaxy, and chosen by the observer. Typically, sky values are measured in 4"-diameter apertures every 2° around the sky circle and at intervals of sky circle plus 4" and sky circle plus 8". The three coangular points are averaged. A plot of intensity vs. position is displayed along with a curve indicating a second-order Fourier-series fit. The observer then may display and choose any order Fourier fit from one (a sine wave) to five. The photometric routines then subtract the sky under each pixel determined from the Fourier sky-fitting equation. The sky fitting function is

$$\text{sky} = \frac{r}{R_0} f(\theta) + a_0 \quad (3)$$

where

$$f(\theta) = \sum_{k=1}^n [a_k \cos(k\theta) + b_k \sin(k\theta)]; \quad (4)$$

$R_0$  is the radius of the middle sky circle;  $r$  and  $\theta$  are the polar coordinates;  $n$  is the order of the fit; and  $a_0$ ,  $a_k$  and  $b_k$  are constants determined by the fit.

## Photoelectric Photometry and Calibration of Photographic Photometry

Photoelectric photometric observations were made on the computer-controlled Mark II photometer on the KPNO 1.3-m telescope. Photoelectric data (U, B, V, R) were obtained on 4 to 8 galaxies, usually E galaxies or early S0s, in the field of each cluster plate except G383. All photoelectric observations were made through apertures with diameters of 18.3 or 36.6. Table 3 lists the galaxies observed photoelectrically. Table 4 gives the filter combinations for each passband.

The photoelectric standard stars, which were primarily in M 67, are given in Sandage (1973). Stars from the equatorial UBV catalog of Landolt (1973) also were observed each run. No systematic differences between UBV transformations were noted using the Sandage and Landolt stars. The Sandage (1973) R band is slightly different from that in the Johnson system (Johnson and Morgan 1951; Johnson 1963). Recently faint standards have been published for the Johnson R (Moffet and Barnes 1979). A number of these stars have been observed along with the usual Sandage standards. A well-defined, color-dependent transformation then was derived to convert our data from the Sandage R system to the Johnson R system (Romanishin 1979, in prep.). The corrections were small -- no greater than 0.04 magnitudes, and typically 0.00 to 0.02 magnitudes.

Table 3. Photoelectric Photometry.

Cluster	Galaxy	Aperture	Date	V	B-V	U-B	V-R
Pisces	N483	36"6	13/12/77	13.63	1.12	0.51	0.88
	N499	36.6	13/12/77	12.83	1.07	0.64	0.93
	N507	18.3	12/12/77	13.23	1.12	0.63	0.86
	N507	18.3	13/12/77	13.24	1.10	0.61	0.90
	N507	36.6	13/12/77	12.67	1.10	0.54	0.88
	N508	18.3	12/12/77	14.27	1.07	0.50	1.01
	N517	36.6	13/12/77	13.44	1.00	0.56	0.85
A262	N687	18.3	12/12/77	13.53	1.09	0.60	0.86
	N687	18.3	13/12/77	13.56	1.06	0.59	0.88
	N687	36.6	13/12/77	13.05	1.06	0.60	0.84
	Z522-33	18.3	12/12/77	15.28	1.06	0.60	0.89
	N703	36.6	13/12/77	13.78	1.15	0.54	0.93
	N708	18.3	13/12/77	14.16	1.15	0.60	0.98
Perseus	N1270	18.3	13/12/77	13.78	1.21	0.71	0.97
	N1270	36.6	13/12/77	13.43	1.22	0.74	0.97
	N1272	18.3	15/12/77	13.98	1.24	0.71	0.99
	N1272	36.6	15/12/77	13.32	1.16	0.72	1.00
	U2673	18.3	13/12/77	14.49	1.17	0.64	0.99
	N1282	18.3	15/12/77	13.53	1.14	0.58	0.91

Table 3.--Continued

Cluster	Galaxy	Aperture	Date	V	B-V	U-B	V-R
A1228	I2744	18.3	13/12/77	14.95	1.11	0.40	0.81
	I2751	18.3	14/12/77	15.09	1.04	0.50	0.86
	I2751	18.3	15/12/77	15.12	1.10	0.46	0.83
	Anon 40	18.3	13/12/77	15.62	1.19	0.49	0.89
A1367	I2951	36.6	9/5/78	14.06	0.95	0.48	0.83
	Z97-85	18.3	12/12/77	15.29	1.06	0.36	0.83
	Z97-85	18.3	9/5/78	15.27	1.05	0.42	0.82
	N3842	18.3	12/12/77	13.64	1.14	0.56	0.84
	N3842	18.3	15/12/77	13.71	1.10	0.62	0.84
	N3860	18.3	9/5/78	14.49	0.82	0.29	0.85
	N3860	36.6	9/5/78	13.88	0.71	0.34	0.78
	N3862	18.3	12/12/77	13.83	1.12	0.51	0.83
	Z97-131	18.3	12/12/77	14.61	1.06	0.42	0.78
	N3873	18.3	12/12/77	13.87	1.08	0.48	0.83
A2199	Anon 53	18.3	9/5/77	15.61	1.05	0.52	0.79
	N6158	36.6	8/5/77	14.00	1.04	0.44	0.80
	Anon 58	36.6	8/5/77	14.76	0.95	0.46	0.87
	N6166	36.6	8/5/77	13.33	1.09	0.51	0.85
	Z224-40	18.3	8/5/77	15.01	1.05	0.48	0.83

Table 3.--Continued

Cluster	Galaxy	Aperture	Date	V	B-V	U-B	V-R
	Z224-40	36.6	8/5/77	14.42	1.04	0.58	0.85
	Anon 68	18.3	9/5/77	14.90	1.08	0.52	0.82
	Anon 68	36.6	9/5/77	14.56	1.01	0.55	0.87

Table 4. Filter Combinations for Photoelectric Observations. -- All observations are with an S20 photocathode.

Photometric Band	Filters
U	Corning 9863 CuSO <sub>4</sub>
B	GG-385 BG-18 Corning 5-57
V	BG-18 GG-495
R	RG-610 KG-3

The photoelectric observations were used to calibrate the photographic photometry and to estimate the accuracy of the latter. Figure 2 shows the U and R magnitudes derived from photoelectric photometry vs. the raw photographic magnitudes within the same size apertures for three typical clusters. The deviations from a  $45^\circ$  line indicate the accuracy of the photographic aperture photometry. The aperture photometry  $1\sigma$  errors are  $\pm 0.04$  in U and  $\pm 0.03$  in R. The R band error estimate includes the uncertainty in the Sandage-to-Johnson system transformation. The photoelectric errors are on the order of .02 in U and .01 in R. The total  $1\sigma$  errors in photographic aperture photometry for both U and R are  $\sim 0.06$ .

No Mark II photoelectric data were available for G383; G383 photoelectric data derive from Sandage (1973). His B, V, R observations include NGC 383 in two aperture sizes and NGC 382 in one aperture. Sandage's data were used to estimate (U-R) as no photoelectric measurements were available. The conversion used to obtain (U-R) from (B-R) will be discussed at the end of this section.

The photometry was corrected for K reddening and for Galactic absorption. K-corrections were calculated from the cluster mean redshifts (Table 2). The K-corrections for U are taken from a study by Pence (1976) who used recent ultraviolet satellite observations. These

Figure 2. Comparisons between Photoelectric Magnitudes and Photographic Raw Magnitudes for Three Typical Clusters.

- a. Pisces U.
- b. Pisces R.
- c. Abell 1367 U.
- d. Abell 1367 R.
- e. Abell 2199 U.
- f. Abell 2199 R.



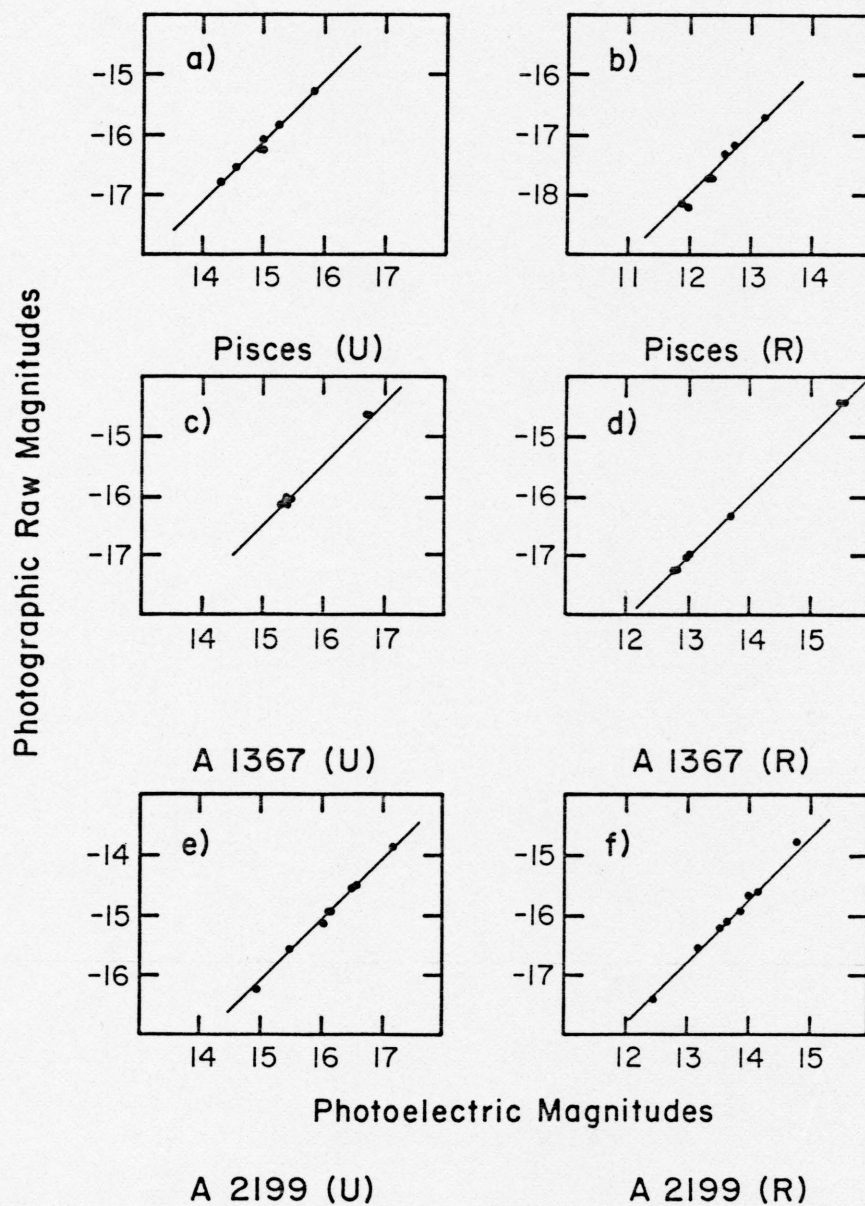


Figure 2. Photoelectric and Photographic Magnitude Comparisons.

corrections are  $<.12$  and are typically  $.07$  mag. The K-corrections for R combine values from works by Whitford (1971) and by Schild and Oke (1971). They are  $<.02$ . The galactic reddening corrections were made using the functions of Sandage (1973). As Sandage does not give the reddening correction in U,  $A_U$ , the value is derived from  $A_B$  using the conversions in Johnson (1965) and Allen (1973).  $A_U$  ranges from zero, for Abell 1228 and Abell 1367, to  $.49$  for Perseus;  $A_R$  is always less than  $.23$ .

The photographic data studied yield direct information for U and R bands only. Frequently, apparent B or V magnitudes were needed; or it was desired to compare (U-B) or (B-R) colors published elsewhere with the (U-R) colors derived herein. For such cases a set of color-color plots was generated from our photoelectric data. The U, B, V, R photoelectric cluster photometry plus some photometry of blue, low-surface-brightness field spirals (Romanishin 1979, in prep.) were plotted in (U-R) vs. (U-B), (U-R) vs. (B-R), (U-R) vs. (U-V), (U-R) vs. (V-R), and (U-R) vs. (B-V). Ninety-six galaxies with a wide range of colors and morphological types were so examined. The (U-B) vs. (U-R) and (B-R) vs. (U-R) plots are reproduced in Figure 3. A polynomial least-squares fit was made to these data. All of the color-color diagrams could be well fit by a first-order polynomial. The additional uncertainty introduced by such

Figure 3. (U-B) vs. (U-R) and (B-R) vs. (U-R) Color-Color Plots. -- A linear least-squares fit is indicated by a solid line. Crude morphological types are indicated as shown in the key.

- a. (U-B) vs. (U-R).
- b. (B-R) vs. (U-R).

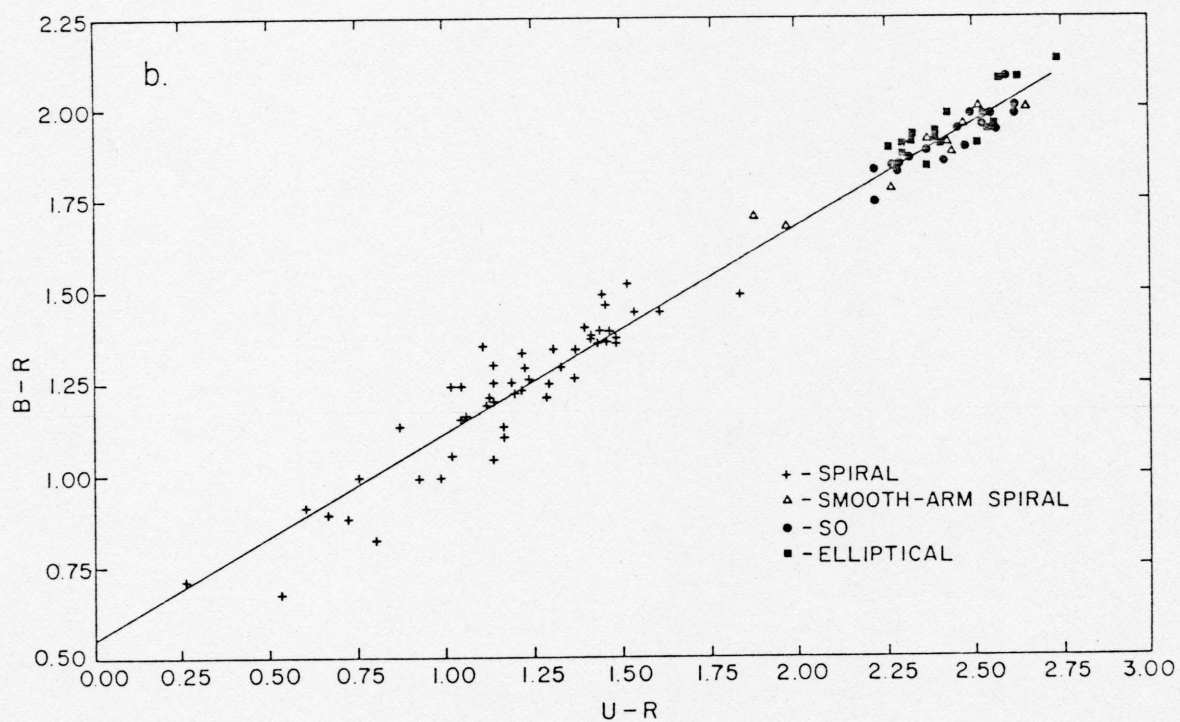
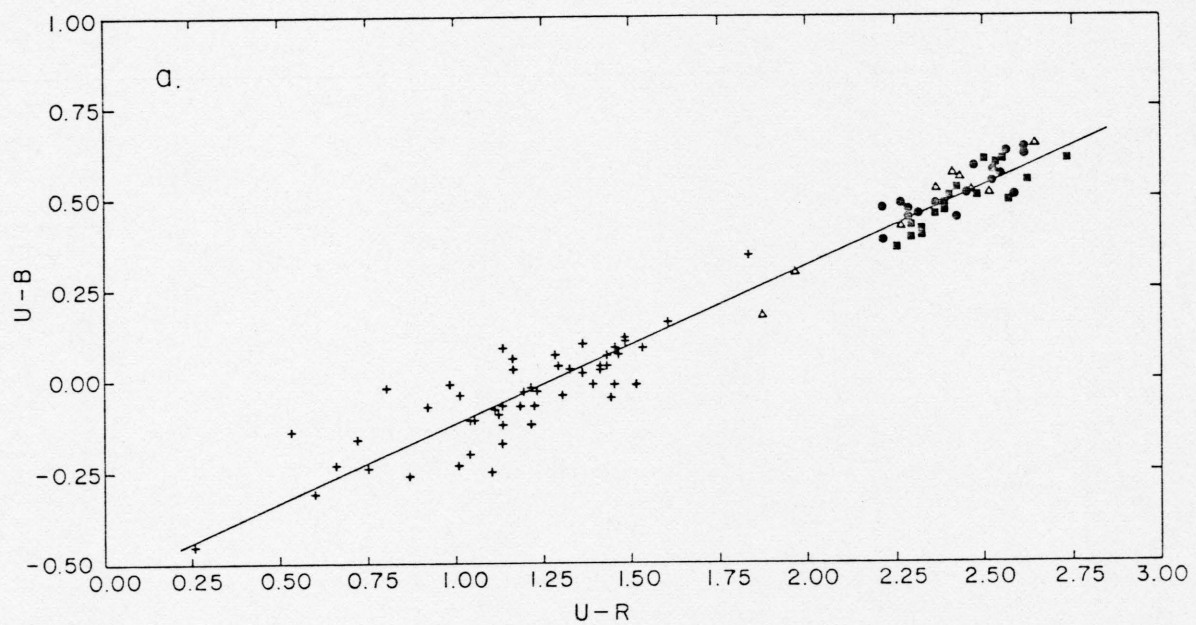


Figure 3. Color-color Plots.

a transformation is 0.06 mag. The two linear-fit functions for the Figure 3 diagrams are

$$(U-B) = .433(U-R) - .549 \quad (5)$$

$$(B-R) = .657(U-R) + .549 \quad (6)$$

### Morphological Typing

Morphological types for all galaxies studied in this investigation, smooth-arm spirals and others, were assigned by L. A. Thompson (1978, pers. comm.). The types assigned were from the de Vaucouleurs modified Hubble system (de Vaucouleurs 1959; de Vaucouleurs and de Vaucouleurs 1976) slightly revised. The revisions to de Vaucouleurs' notation are as follows:  $R_O$  indicates an outer ring;  $R_D$  -- ring around disk;  $R_N$  -- ring around nucleus; + or - applied to rings -- strong or weak rings, respectively. In addition the author added the following designations after Thompson's assignments were complete: initial M indicates a good smooth-arm spiral; initial m -- fair smoothy. The distinctions between "good" and "fair" are discussed at the beginning of this chapter. All other notations are as in de Vaucouleurs (1959).

Thompson's primary criteria for distinguishing the classes of spirals (i.e., Sa, Sb, Sc, Sd) were the eye-estimate disk to bulge ratios, with Sa's having smaller D/B



than Sb's, etc., and the degree of arm winding, with Sa's having more tightly wound arms than Sb's, etc.

At present, morphological typing remains a highly subjective exercise. It was due to this subjectivity and possible bias, that the author wished independent morphological assignments. A real need exists to quantify morphological types, especially within the spiral and S0 groupings, by not only stating the criteria for each class, but by assigning numerical ranges to said criteria. Some work has been done toward this end (e.g., Wakamatsu 1976; Strom, in press), but much effort yet remains.

It might be noted that, in several instances, what the present study has called a smooth-arm spiral (m or M) is classified traditionally (e.g., Thompson's assigned classification) as S0 or, more commonly, SB0. The author's assumption is that any galaxy exhibiting arm structure can be used as a candidate for a smooth-arm spiral. As will be seen, these S0 and SB0 galaxies with evidence of partial or "degenerate" arms could represent an interesting phase in spiral-to-S0 evolution.

#### Image-tube Direct Photography

We consider as a working hypothesis that smooth-arm spiral galaxies may be spirals from which the gas has been removed. Our sample clusters, within which the studied galaxies reside, are primarily x-ray-emitting clusters.

The x-ray emission implies the presence of a hot intracluster gas. Our working hypothesis may be extended to suggest that the primary gas-removal mechanism is stripping via a hot intracluster medium. An immediate question comes to mind: do smooth-arm spirals occur in the field?<sup>2</sup> If so, with what frequency? It would seem unlikely that no smooth-arm spirals are present in the field or in small associations. The field smooth-arm spirals could represent those spirals that have exhausted their disk gas or in which gas has been self-removed, for example by strong galactic winds. However, if smooth-arm spirals arise primarily from external sources of gas removal, then the frequency of cluster smoothies compared to the frequency of field smoothies should be larger. Studies of field and cluster S0s have found the nearby field S0 population to make up 10% of the total; whereas in clusters S0s represent 30% to 50% of the total number of galaxies (Dressler, in press), or increases by factors of 3 to 5. A similar or greater increase might be expected in the frequency of cluster spirals compared with field smooth-arm spirals. The greater increase might be expected if cluster stripping has not been continuous

---

<sup>2</sup>"Field" will be used to mean lower-density regions of superclusters in addition to its usual definition of truly isolated galaxies. (i.e., "Field" galaxies are galaxies that are not in clusters or in regions of sufficiently high galaxy density that a hot, intergalactic medium may exist.)

over the lifetime of the Universe, but has only commenced in the past few billion years.

A search was made for smooth-arm spirals in low-density regions. The Palomar Sky Survey O plates were searched to find field-smoothy candidates. The search was made of all Sky Survey plates with declinations  $\geq +30^\circ$ . "Low-density" was defined to be any region not in or near ( $< 3 r_{\text{cluster}}$ ) a cluster or dense group. Due to the relatively low spatial resolution and, in particular, the high grain noise, one cannot distinguish between smooth-arm spirals and anemics. Candidates selected from the Sky Survey were photographed with an image-tube direct system on the KPNO #1 - 0.9 meter telescope. This system at  $f/7.5$  gives a plate scale of 30 arcsec/mm. The Sky Survey has a plate scale of 67 arcsec/mm. The use of baked IIIa-J plates, rather than 103a-O plates as in the Sky Survey, decreases the granularity by a factor of  $\sqrt{2}$  (implying a factor of 4 increase in information content per unit plate area) and at the same time increases the dynamic range (Eastman Kodak Company 1973).

Two additional candidate smooth-arm spirals were observed with the Hale Observatories' 1.2-m Schmidt telescope and baked IIIa-J plates. Table 5 lists the galaxies observed, morphological types, and their "smoothness" at the resolution of the plates. As can be seen in Table 5



Table 5. Photographic Record of Candidate Smooth-arm Spirals in the Field or in Small Associations.-- Morphological types are given in the de Vaucouleurs' revised Hubble system (de Vaucouleurs 1959) as cited in the Uppsala General Catalog (Nilson 1973) except as noted.

Name	R.A. (1950)	Dec. (1950)	Morphological Type	Smooth?
N2273	06 45.6	+60 54	SB(r)a	No
Z285-13	06 58.2	+62 50	SB(r)0+ <sup>a</sup>	Yes
U3723	07 07.5	+34 30	SB0 <sup>b</sup>	Yes:
Z181-2	09 11.3	+36 18	(R')SB(s)a	Yes
N2859	09 21.3	+34 44	(R)SB(r)0+	Yes
Z181-50	09 27.1	+36 54	SB(r)ab <sup>a</sup>	No
N2971	09 40.7	+36 24	SB(r)b	No
N6085	16 10.5	+29 30	Sa <sup>b</sup>	No
U10712	17 05.4	+31 30	(R)SABa	No

a. de Vaucouleurs revised Hubble type determined by the author.

b. Hubble type as given in the Uppsala General Catalog.

the number of smoothy candidates actually surveyed is small. Of thirteen nights available for this aspect of the project, one full night and two half nights were usable.

The significance of these data will be discussed further in the next chapter.

### Spectroscopy

Spectra were obtained of a few smooth-arm spirals. The plates were taken with the white image-tube spectrograph on the KPNO #1 - 0.9 meter telescope at a reciprocal dispersion of  $141 \text{ \AA/mm}$ . The purpose of the spectroscopy was twofold: to search for emission lines indicating the presence of excited gas in the galaxy, and to determine redshifts to facilitate the radio observing.

The objects observed and spectral lines found are catalogued in Table 6. Redshifts were determined using a computer program developed by G. R. Gisler (1979, in prep.) that cross-correlates the observed spectrum with a template spectrum.

### 21-cm Observations

Neutral hydrogen observations of smooth-arm spirals made by Sullivan, Schommer and Bothun (1979, pers. comm.) in the course of surveys of galaxy clusters have provided no H I detections. It was felt that detections or very low upper limits were crucial to the understanding of

Table 6. Optical Spectroscopic Data.

Object	Spectrum #	UT Date	Redshift	Emission Lines	ID
Z97-101	4997b	30/4/79	$.0214 \pm .0003$	6008Å 6034 6080	HeI $\lambda$ 5875
Z97-105	4997a	30/4/79	$.0184 \pm .0003$		
NGC3857	4997c	30/4/79	$.0191 \pm .0003$		
UGC10404	4999b	30/4/79	$.0266 \pm .0002$	3822 5089 5144	[OII] $\lambda$ 3727 [OIII] $\lambda$ 4959 [OIII] $\lambda$ 5007
Z224-40	4999c	30/4/79	$.0322 \pm .0003$	3847	[OII] $\lambda$ 3727

these galaxies, since we hypothesize that they are disk galaxies containing little or no gas. Therefore observing time was requested and obtained on the 305-m telescope of the Arecibo Observatory.

The observations were made 27 November through 11 December 1978 and 2 through 8 June 1979. The dual-circular-polarization 1420 MHz line feed was lowered to center its response at 1403.8 MHz. The two signals were recorded independently with the 1008-channel autocorrelation spectral-line receiver and added together in the reductions. Each of the resultant 504 channels had a channel spacing of 19.531 kHz, for an effective velocity coverage of  $\sim 2100$  km/sec.

On-source, off-source position switching was used. In this procedure the object is tracked for five minutes; then an equal-length track of blank sky is made through exactly the same range of azimuth and zenith angle. This method of observing minimizes differential contributions to the system temperature from the sky and from ground pickup.

The observing frequency was centered on the optically-determined heliocentric velocity, or in those few cases where no redshift was known prior to the observations, the frequency was centered near the cluster mean velocity. In all cases the galaxies without specifically known optical

redshifts were actively-star-forming cluster spirals measured for the sake of comparison with the smooth spirals.

In reduction, corrections were made for zenith angle, frequency response, and the different gain of the two polarization channels. Noise-source calibration measurements were taken 5 to 15 times per observing session and were converted directly into Jy using observations of the continuum sources 3C 67.0, 3C 75.0, 3C 76.1, 3C 208.1, 3C 287.0, 3C 466 and CTA 21 (Bridle et al. 1972).

The off-source scan was subtracted point-by-point from the on scan. The result was divided by the off scan. Baselines were fitted using a second-order polynomial and then subtracted from the data. The data were then Hanning smoothed three times and examined for H I emission features.

Neutral hydrogen mass in solar-mass units was computed from

$$M_{\text{HI}} = 2.36 \times 10^5 D^2 \Sigma S_{\text{v}} dv, \quad (7)$$

where  $D$  is the distance to the galaxy in Mpc and  $\Sigma S_{\text{v}} dv$  is the total line flux in Jy-km/sec (Roberts 1969). All galaxies are assumed to be unresolved by the telescope (FWHM of beam approximately 3.2 arcminutes); the galaxies all have optical major-axis lengths less than 2.4 arcmin. By far the worst case for not meeting the criterion for

non-resolution is NGC 3861. For this galaxy the flux is underestimated by  $\sim 30\%$ .

H I upper limits for those galaxies that remained undetected were determined by using equation (7) and by assuming a rectangular profile with a line height of  $3\sigma$ , where  $\sigma$  is the standard deviation of the noise across the assumed line width, and assuming a line width of  $(500 \sin i)$  km/sec (Roberts 1978), where  $i$  is the inclination of the galaxy. The inclination was determined from  $i = \cos^{-1}(b/a)$ , where  $b/a$  is the minor-to-major-axis ratio.

The results of the observations are listed in Table 7. The columns are as follows:

1. Name of the galaxy. Designations are given in NGC numbers when available, otherwise the UGC designation is tabulated.
2. The cluster or group with which the galaxy is associated.
3. The morphological type of the galaxy as determined by L. Thompson in the de Vaucouleurs revised Hubble system.
4. The total integration time spent on the object at Arecibo. Total on plus off time is twice that listed.
5. The distance in Mpc to the cluster based on mean redshifts in the literature and using  $H_0 = 75 \text{ km sec}^{-1} \text{ Mpc}^{-1}$ .
6. The optical heliocentric velocity in km/sec of each galaxy. If a central velocity different from the optical

Table 7. Results of Neutral Hydrogen Observations of Five Smooth-arm Spirals and Four Non-smooth Cluster Galaxies.

Object (1)	Cluster (2)	Type (3)	t (4)	D (5)	V <sub>OPT</sub> (6)	V <sub>HI</sub> (7)	m <sub>B</sub> (8)	U-R (9)	i (10)	ΔV (11)	ES <sub>v</sub> dv (12)	σ (13)	M <sub>HI</sub> (14)	M <sub>HI</sub> /L <sub>B</sub> (15)
Smooth-arm Spirals														
NGC 399	G383 (Pisces)	SBO+(R <sub>D</sub> R <sub>O</sub> )	35	71	5167	(5167)	14.48	2.26	45°	(354)		1.80	<2.3×10 <sup>9</sup>	<0.18
NGC 495	Pisces	SBc	160	59	4114	(4114)	14.45	2.25	40	(321)		0.55	<3.6×10 <sup>8</sup>	<0.039
UGC 1344	A262	SBab	75	67	4428	4155:	13.66	2.08	45	103:	0.34:	1.19	≤3.6×10 <sup>8</sup>	≤0.015
UGC 1350	A262	SABc	160	67	5350	4975	14.24	2.06	45	252	0.48	0.66	5.0×10 <sup>8</sup>	0.036
NGC 3860	A1367	SAb	120	85	5461	(5461)	14.24	1.97	55	(410)		0.60	<1.2×10 <sup>9</sup>	<0.055
Non-smooth Cluster Galaxies														
UGC 1347	A262	SAc	30	67	4996 (4800)	5524	13.67	1.53	25	144	3.4	1.80	3.5×10 <sup>9</sup>	0.150
NGC 710	A262	SAc	15	67	(4800)	(4800)	14.09	1.35	50	(383)		2.80	<4.1×10 <sup>9</sup>	<0.21
UGC 6697	A1367	Sd:(edge)	40	85	6698 (6000)	6746	14.41	1.20	80?	>275	>2.0	1.19	>3.3×10 <sup>9</sup>	>0.172
NGC 3861	A1367	SABd(R <sub>N</sub> )	10	85	5015	5076	13.47	1.83	55	486	4.8	2.04	8.1×10 <sup>9</sup>	0.178

velocity was used it is given in parentheses. If no optical velocity was known the central velocity alone is given in parentheses.

7. The radial velocity in the 21-cm radio emission line as determined by this study. If no emission line was seen, the assumed velocity used in the reductions is given in parentheses.

8. The total apparent B magnitude of the galaxies. Magnitudes were integrated to the  $26.5 \text{ mag/arcsec}^2$  isophote as discussed in the section on photographic and photoelectric photometry.

9. Integrated (U-R) color to the  $B = 26.5 \text{ mag/arcsec}^2$  isophote.

10. The inclination,  $i$ , of the galaxy.

11. The width in km/sec of the 21-cm emission line at 20% of the peak. If no line was detected a width of  $(500 \sin i) \text{ km/sec}$  is assumed in the upper-limit calculations.

12. The flux integral,  $\Sigma S_{\nu} dv$ , in Jy-km/sec.

13. The standard deviation,  $\sigma$ , (root mean square of the deviation) in mJy of the noise, taken over a typical section of spectrum of width equal to the real or assumed line width. Upper line-height limits for non-detections are set at  $3\sigma$ .

14. The neutral hydrogen mass or mass upper limit in solar units.



15. The neutral hydrogen mass to B luminosity ratio in solar units. The absolute B magnitude of the sun is taken to be 5.48 (Allen 1973).

## CHAPTER 3

### RESULTS

The study of smooth-arm spiral galaxies has involved many different kinds of observations. This chapter shall present the results of these observations with little attempt to collate data from different fields. Analysis and interpretation follow in the final chapter.

#### The Photographic Photometry

##### Annular-aperture Photometry

The annular-aperture photographic photometry for all the galaxies considered in this study is presented in Table 8. In addition, the galaxies' morphological types in modified de Vaucouleurs notation, as described in the section on morphological typing, are given, as are U and R magnitudes and colors in a circular aperture of radius equal to the radius of the outer dimension of the largest annular aperture used. An annular-aperture color is not given if the average U magnitude/arcsec<sup>2</sup> is greater than or equal to 26, or if nearby galaxies or bright stars contaminate the aperture.

Table 8. Annular- and Circular-aperture Photographic Photometry. -- Annular apertures, given by radii, are in magnitudes of U-R. Circular apertures (radius explained in text) are headed by passband names.

Object	R.A. (1950)	Dec. (1950)	Type	2"-5"	5"-10"	7.5"-20"	10"-30"	U	R	U-R
<u>G 383</u>										
U 679	01 04 17.8	+32 07 21	Sm	1.37	1.23	1.07	0.92	16.38	15.31	1.07
N 374	01 04 19.9	+32 31 40	MSA0/a(R <sub>D</sub> )	2.23	2.37	2.38	2.38	15.01	12.66	2.35
N 379	01 04 29.9	+32 15 13	E+	2.43	2.36	2.40	2.39	14.64	12.25	2.39
N 380	01 04 31.9	+32 12 57	SA0	2.21	2.36	2.39	2.36	14.55	12.24	2.31
N 382	01 04 38.2	+32 08 13	E	2.30	2.43	2.44	2.44	14.66	12.26	2.40
N 383	01 04 39.3	+32 08 44	S0-	2.40	2.36	2.44	2.45	14.03	11.61	2.42
N 384	01 04 39.3	+32 01 32	E+	2.18	2.25	2.24	2.21	14.79	12.57	2.22
N 385	01 04 41.5	+32 03 10	S0-	2.17	2.35	2.17	2.09	15.98	13.76	2.22
N 399	01 06 13.1	+32 22 04	MSB0+(R <sub>D</sub> R <sub>O</sub> )	2.32	2.29	2.31	2.27	15.12	12.82	2.30
N 403	01 06 27.9	+32 29 09	mSAB0+(R <sub>O</sub> )	2.15	2.24	2.31	2.31	14.47	12.19	2.28
U 714	01 06 28.1	+31 53 06	SAb	1.62	1.44	1.36	1.33	14.61	13.22	1.39
Z501-105	01 06 34.2	+32 27 23	SABc	1.81	1.44	1.51	1.43	15.21	13.69	1.52
Z501-107	01 06 47.3	+31 54 25	SO+: (edge)	1.98	1.87	1.91	1.90	16.07	14.15	1.92
U 724 <sup>a</sup>	01 07 13.3	+32 06 09	SAab pec	1.63	1.39	1.08	1.41	14.21	12.71	1.50
<u>Pisces</u>										
I 1679	01 18 55.6	+33 13 56	MSB0+(R <sub>D</sub> <sup>+</sup> )	2.12	2.05	1.96	1.94	16.10	14.08	2.02
I 1680	01 19 02.4	+33 01 17	SA0+ pec	2.22	1.94	2.05	1.90	15.69	13.58	2.11
N 483	01 19 07.3	+33 15 35	MSAB0(R <sub>D</sub> <sup>-</sup> )	2.41	2.17	2.13	2.10	14.94	12.65	2.29
I 1682	01 19 24.4	+32 59 56	mS0/a	2.25	1.96	2.03	2.03	15.40	13.25	2.15
Z502-55	01 19 45.2	+32 50 32	MSB0+(R <sub>D</sub> <sup>+</sup> )	1.85	1.81			16.66	14.81	1.85

Table 8. Annular- and Circular-aperture Photographic Photometry. -- Continued

Object	R.A. (1950)	Dec. (1950)	Type	2"-5"	5"-10"	7.5"-20"	10"-30"	U	R	U-R
Anon 0	01 20 04.0	+33 09 10	SABd pec	2.18	2.14	2.04	1.99	16.13	14.03	2.10
N 494 <sup>a</sup>	01 20 06.2	+32 54 47	SAb	2.33	2.17	2.07	2.01	14.36	12.25	2.11
N 495	01 20 06.9	+33 12 38	MSBc	2.34	2.31	2.19	2.15	14.93	12.66	2.27
N 496 <sup>a</sup>	01 20 22.3	+33 16 06	SAab	1.41	1.40	1.21	1.17	14.41	13.18	1.23
N 499	01 20 22.4	+33 11 58	SA0-	2.63	2.40	2.28	2.22	14.00	11.60	2.40
Anon 1	01 20 31.2	+33 05 12	I	0.50	0.40	0.46		17.02	16.55	0.47
N 501	01 20 33.2	+33 10 20	SA0	2.24	2.22	2.11		16.06	13.78	2.28
N 504	01 20 38.9	+32 56 37	S0+pec (edge)	2.42	2.15	2.09	2.05	15.04	12.75	2.29
N 503	01 20 39.4	+33 04 17	mSB0+	2.14	2.06	2.04	2.03	15.62	13.50	2.12
N 507 <sup>a</sup>	01 20 50.8	+32 59 42	SA0 pec	2.51	2.20	2.20	2.16	13.75	11.47	2.28
N 508	01 20 51.5	+33 01 12	SA0+	2.31	2.37	2.27	2.20	14.80	12.52	2.28
I 1690	01 21 00.5	+32 53 44	SA0 (edge)	2.13	2.11	2.01		15.94	13.80	2.14
Z502-72	01 21 09.3	+33 03 10	mSB0+	2.32	2.13	2.00	1.91	15.76	13.66	2.10
Anon 2	01 21 09.9	+33 04 15	mS0pec (R <sub>D</sub> <sup>+</sup> )	1.85	1.89	1.80		16.93	15.09	1.84
Anon 3	01 21 36.4	+33 08 49	SB0+ (R <sub>D</sub> <sup>-</sup> )	1.97	1.92	1.78		16.59	14.67	1.92
N 515	01 21 49.0	+33 10 09	SB0	2.34	2.25	2.14	2.08	14.89	12.63	2.26
N 517	01 21 54.4	+33 12 46	SA0	2.34	1.98	1.94	1.86	14.63	12.52	2.11
<u>A 262</u>										
Anon 4	01 47 28.2	+36 05 33	S0 (edge)	2.07	2.00	1.91		16.65	14.62	2.03
N 687	01 47 37.1	+36 07 24	SA0-	2.20	2.23	2.23	2.22	14.08	11.88	2.20
Z522-25	01 49 06.6	+35 53 04	SBcd (R <sub>N</sub> )	1.85	1.61	1.57	1.63	15.41	13.76	1.65
N 700	01 49 16.5	+35 51 03	SB0+:	2.31	2.23	2.19	2.22	15.90	13.60	2.30
Z522-30	01 49 20.7	+35 47 25	SAB0-	2.21	2.20	2.07	1.99	15.65	13.42	2.23

Table 8. Annular- and Circular-aperture Photographic Photometry. -- Continued

Object	R.A. (1950)	Dec. (1950)	Type	2"-5"	5"-10"	7.5"-20"	10"-30"	U	R	U-R
Z522-33	01 49 36.3	+35 52 09	E	2.34	2.34	2.19	2.00	15.90	13.62	2.28
U 1344 <sup>a</sup>	01 49 38.2	+36 15 17	MSABc	2.19	2.11	1.93	1.53	13.80	12.04	1.76
N 703	01 49 43.3	+35 55 31	SA0-	2.44	2.37	2.27	1.85	14.74	12.96	1.78
N 705 <sup>a</sup>	01 49 45.2	+35 53 52	S0: (edge)	2.35	2.26	2.27	2.29	14.76	12.42	2.34
U 1347 <sup>a</sup>	01 49 49.2	+36 22 21	SAC	2.08	1.53	1.21	1.11	13.70	12.42	1.28
N 708 <sup>a</sup>	01 49 50.0	+35 54 20	E+	2.81	2.57	2.28	2.20	14.23	11.80	2.43
N 709	01 49 54.2	+35 58 38	SA0	2.13	2.10			15.93	13.72	2.21
N 710	01 49 57.6	+35 48 27	SAC	1.58	1.47	1.31	1.21	14.12	12.80	1.32
U 1350 <sup>a</sup>	01 50 00.7	+36 16 00	MSBab	2.21	2.26	2.19	2.13	14.91	12.73	2.18
Anon 5	01 50 03.1	+35 51 41	S0+ pec	2.16	2.18	2.13		16.72	14.53	2.19
<u>Perseus</u>										
I 310	03 13 25.3	+41 08 30	E+	2.31	2.34	2.23	2.18	14.43	12.16	2.27
U 2626	03 13 41.9	+41 10 24	S0+ (edge)	2.28	2.09	1.94	1.83	15.40	13.21	2.19
Anon 6	03 13 55.7	+41 15 09	SB0/a	1.67	1.98	1.83		16.41	14.44	1.97
Anon 7	03 13 59.4	+41 12 09	SA0	2.19	2.12	1.75	1.62	15.10	13.13	1.97
Anon 8	03 13 59.7	+41 14 18	S0- (edge)	1.99	2.02			17.35	15.30	2.05
N 1260	03 14 09.2	+41 13 20	SA0 pec	2.34	2.16	2.13	2.22	14.67	12.39	2.28
Anon 9	03 14 11.2	+41 11 34	mSAb	1.96	1.83	1.64	1.57	15.09	13.35	1.74
Anon 10	03 14 14.1	+41 13 44	MSBd	2.01	2.01	1.85	1.64	15.90	14.07	1.83
Anon 11	03 14 39.4	+41 18 54	SB0	2.03	1.99	1.72		16.27	14.32	1.95
N 1264	03 14 41.3	+41 20 17	mSB0 ( $R_N, R_D^-$ )	2.38	2.13	2.07	2.02	15.15	12.99	2.16
Z540-89	03 15 17.7	+41 17 44	SA0+	2.19	2.15			16.15	13.93	2.22



Table 8. Annular- and Circular-aperture Photographic Photometry. -- Continued

Object	R.A. (1950)	Dec. (1950)	Type	2"-5"	5"-10"	7.5"-20"	10"-30"	U	R	U-R
N 1267	03 15 26.5	+41 17 09	SA0	2.58	2.38	2.27	2.19	14.65	12.25	2.40
Anon 12	03 15 26.5	+41 19 48	S0-	2.21	2.02			17.42	15.27	2.15
N 1268	03 15 26.8	+41 18 27	MSAc	1.75	1.76	1.60	1.53	14.65	13.02	1.63
Anon 13	03 15 29.1	+41 14 48	S0 (edge)	2.16	2.00			16.88	14.74	2.14
Anon 14	03 15 29.9	+41 15 30	dS pec(edge)	1.24	1.40			18.55	17.23	1.32
N 1270	03 15 39.8	+41 17 18	E	2.60	2.49	2.40	2.38	14.78	12.17	2.61
Anon 15	03 15 44.6	+41 19 22	S0-:	1.77	1.56			18.11	16.35	1.76
N 1271	03 15 53.2	+41 10 19	S0 (edge)	2.41	2.23	2.05	1.99	15.41	13.09	2.32
N 1272 <sup>a</sup>	03 16 02.9	+41 18 34	E+	2.59	2.44	2.32	2.19	14.27	11.88	2.39
Anon 17	03 16 04.0	+41 14 53	S0 (edge)	2.38	2.40			16.41	13.97	2.50
N 1273	03 16 08.2	+41 21 34	SA0	2.30	2.18	2.15	2.10	14.72	12.43	2.29
Anon 18	03 16 18.8	+41 18 18	SAB0	2.23	2.23			16.79	14.47	2.32
Anon 19	03 16 21.9	+41 08 54	S0	2.24	2.33			16.65	14.31	2.34
N 1274	03 16 22.1	+41 22 04	SA0	2.34	2.30	2.18	2.24	15.49	13.07	2.42
Anon 20	03 16 24.2	+41 25 12	S0 (edge)	1.99	1.47			17.40	15.48	1.92
Anon 21	03 16 26.3	+41 05 51	SA0	2.34	2.26	2.02		15.84	13.58	2.26
Anon 22	03 16 28.6	+41 05 23	E+	2.17	1.93	1.63		16.68	14.75	1.93
Anon 23	03 16 29.1	+41 24 57	E+	2.32	2.19	2.11	2.05	15.62	13.36	2.26
N 1275 <sup>a</sup>	03 16 29.6	+41 19 51	E pec	1.53	1.62	1.65		13.18	11.45	1.73
N 1277	03 16 32.9	+41 23 34	S0-	2.57	2.24	2.25	2.15	15.08	12.61	2.47
Anon 24	03 16 34.3	+41 25 41	S0-	2.02	1.85	1.79		16.84	14.90	1.94
Anon 25	03 16 34.8	+41 07 18	SB0 (R <sub>D</sub> )	2.27	2.36	2.20	2.15	15.42	13.12	2.30

Table 8. Annular- and Circular-aperture Photographic Photometry. -- Continued

Object	R.A. (1950)	Dec. (1950)	Type	2"-5"	5"-10"	7.5"-20"	10"-30"	U	R	U-R
N 1278	03 16 35.4	+41 22 58	E	2.58	2.45	2.43	2.39	14.53	12.02	2.51
Anon 28	03 16 42.2	+41 22 24	SB0	2.08	2.17	2.01		16.08	13.84	2.24
U 2673	03 16 43.6	+41 04 14	S0-	2.41	2.32	2.22	2.16	14.94	12.64	2.30
Anon 28	03 16 44.2	+41 19 44	E	2.21	1.99			17.27	15.04	2.23
Anon 30	03 16 51.8	+41 10 15	S0+(edge)	1.55	1.68	1.69	1.73	15.94	14.30	1.64
N 1282	03 16 53.8	+41 11 12	E+	2.26	2.20	2.10	2.02	14.51	12.31	2.20
Anon 31	03 16 55.0	+41 06 24	S0 pec	1.71	1.72			16.91	15.16	1.75
N 1283	03 16 57.1	+41 13 06	SA0	2.40	2.32	2.30	2.33	15.36	12.93	2.43
Anon 32	03 16 59.1	+41 10 07	S0-	2.08	2.19	2.16		16.55	14.38	2.17
Anon 33	03 17 02.5	+41 11 37	MSAd( $R_N$ )	2.12	2.08	2.00	1.68	15.91	13.95	1.96
				<u>A 1228</u>						
Anon 34	11 17 25.0	+34 24 06	MSB0	2.40	2.32			17.29	14.96	2.33
U 6347	11 17 38.9	+34 22 13	SAA	2.16	2.13	1.74	1.56	15.50	13.57	1.93
I 2735	11 18 28.8	+34 37 24	Sm	1.60	1.56			17.16	15.55	1.61
I 2738	11 18 41.4	+34 37 52	E	2.45	2.25	2.10	2.08	15.36	13.12	2.24
Anon 35	11 18 42.5	+34 28 56	SAb	1.69	1.65			17.05	15.35	1.70
Z185-43	11 18 45.2	+34 43 37	SA0	2.28	2.12	1.98	1.74	15.97	13.87	2.10
Anon 36	11 18 52.5	+34 28 10	MSBb	2.21	2.22	2.29		17.08	14.86	2.22
I 2744	11 19 00.9	+34 38 12	E	2.40	2.30	2.32	2.32	15.20	13.13	2.37
Anon 37	11 19 01.2	+34 34 52	SBm	1.19	1.11	1.39	1.40	15.62	14.29	1.33
Z185-46	11 19 21.7	+34 35 20	MSAab	2.25	2.03	1.88	1.79	15.52	13.47	2.05
I 2751	11 19 25.8	+34 38 27	E	2.29	2.21	2.00	1.81	15.98	13.85	2.13
Anon 38	11 19 32.9	+34 33 23	SABc pec	1.77	1.61	1.76		16.60	14.85	1.75

Table 8. Annular- and Circular-aperture Photographic Photometry. -- Continued

Object	R.A. (1950)	Dec. (1950)	Type	2"-5"	5"-10"	7.5"-20"	10"-30"	U	R	U-R
Anon 39	11 19 54.4	+34 40 05	SAb	1.79	1.61	1.45		16.36	13.84	2.52
U 6393	11 20 12.2	+34 36 56	MSBd	2.30	2.14	2.03	1.98	15.20	13.06	2.14
Anon 40	11 20 17.8	+34 34 00	S0-	2.31	2.39			17.01	14.66	2.35
U 6397 <sup>a</sup>	11 20 20.7	+34 46 19	Sb (edge)	2.34	2.25	2.02	1.98	15.32	13.14	2.18
Anon 41	11 20 24.2	+34 37 30	mdS0	2.20	2.10			17.44	15.26	2.18
Z185-53	11 20 29.4	+34 45 51	Sc (edge)	1.84	1.63	1.47	1.43	15.60	13.97	1.63
Anon 42	11 20 32.9	+34 39 32	SAc	1.57	1.16	1.39	1.51	16.23	14.81	1.42
<u>A 1367</u>										
U 6680	11 40 26.5	+19 55 37	SABb(R <sub>N</sub> )	2.29	2.12	1.98	1.95	15.66	13.59	2.07
U 6683	11 40 40.6	+20 01 34	S0/a (edge)	2.27	2.26	2.19	2.18	15.77	13.50	2.27
I 2951 <sup>a</sup>	11 40 49.0	+20 01 39	MSAb	2.20	2.23	2.14	2.09	15.06	12.90	2.16
Z97-83	11 40 55.6	+19 54 19	SABc	1.99	1.71	1.54	1.48	15.36	13.60	1.76
Z97-85	11 41 01.4	+19 52 55	E+	2.18	2.15	2.11	2.07	16.14	13.99	2.15
Z97-86	11 41 11.1	+20 19 00	S0 (edge)	2.13	2.26	2.08		16.34	14.14	2.20
U 6697 <sup>a</sup>	11 41 13.2	+20 14 48	Sd: (edge)	1.44	0.89	0.97	0.96	14.08	13.07	1.01
N 3837	11 41 20.8	+20 10 19	E+	2.37	2.41	2.34	2.30	14.90	12.57	2.33
Z97-90	11 41 21.9	+20 13 52	E	2.34	2.36	2.32		15.98	13.62	2.36
N 3844	11 41 25.2	+20 18 25	S0/a? (edge)	2.27	2.31	2.27	2.23	15.40	13.13	2.27
N 3842	11 41 26.5	+20 13 38	S0-	2.50	2.43	2.42	2.38	14.16	11.76	2.40
N 3841	11 41 26.5	+20 14 58	E	2.26	2.27	2.21	2.16	15.25	13.02	2.23
N 3845	11 41 29.9	+20 16 26	SAB0 pec	2.15	2.26	2.12	2.00	15.52	13.35	2.17
Z97-101	11 41 43.4	+20 07 21	MSB0/a	2.38	2.43	2.41	2.26	15.58	13.22	2.36



Table 8. Annular- and Circular-aperture Photographic Photometry. -- Continued

Object	R.A. (1950)	Dec. (1950)	Type	2"-5"	5"-10"	7.5"-20"	10"-30"	U	R	U-R
N 3851	11 41 44.8	+20 15 31	E	2.29	2.22	2.10	2.02	15.71	13.47	2.24
Z97-105	11 41 45.2	+20 06 13	MSB0/a	2.35	2.39	2.41		16.04	13.65	2.39
Z97-110	11 41 49.6	+20 06 20	SA0	2.19	2.29	2.34		16.30	14.03	2.27
Z97-109	11 41 52.8	+20 00 45	E?	2.13	2.03	2.06		16.29	14.19	2.10
Z97-115	11 42 12.0	+20 09 14	SA0+	2.26	2.18	2.13		16.16	13.95	2.21
Z97-119	11 42 12.5	+19 57 58	SAB0/a ( $R_N$ )	1.95	1.96	1.93	1.84	16.10	14.18	1.92
Anon 43	11 42 12.6	+19 51 31	E	2.06	2.02	1.97		16.80	14.73	2.07
N 3860 <sup>a</sup>	11 42 13.7	+20 04 21	mSAb	1.97	1.92	1.92	1.93	14.65	12.68	1.97
N 3857	11 42 14.8	+19 48 37	MSAb	2.30	2.39	2.37	2.31	15.57	13.24	2.33
Z97-118	11 42 16.7	+19 53 15	SB0+ pec	2.08	2.15	2.01		16.59	14.45	2.14
Z97-124	11 42 21.5	+20 00 35	SAB0+	2.34	2.44	2.36	2.16	15.80	13.51	2.29
Anon 45	11 42 26.3	+20 02 29	S0-	1.76	1.72			17.83	16.08	1.75
I 2955	11 42 28.4	+19 53 54	E	2.35	2.41	2.39	2.40	15.51	13.10	2.41
N 3861 <sup>a</sup>	11 42 28.4	+20 15 05	SABd ( $R_N$ )	2.48	2.28	1.80	1.66	14.30	12.34	1.96
Anon 46	11 42 29.3	+19 57 34	E	2.14	2.05			17.28	15.10	2.18
N 3862	11 42 29.5	+19 53 02	S0-	2.51	2.46	2.47	2.45	14.60	12.19	2.41
Anon 47	11 42 20.3	+20 04 13	E	2.28	2.23			18.35	16.03	2.32
N 3861 B	11 42 31.5	+20 14 40	Sb: ( $R_N$ )	1.94	1.74	1.57		15.78	14.08	1.70
Anon 48	11 42 38.3	+20 02 01	S0/a pec	1.98	1.89	1.76		16.88	15.01	1.87
Z97-131	11 42 39.4	+20 07 23	S0-	2.23	2.26	2.15	2.10	15.44	13.22	2.22
N 3864	11 42 40.2	+19 40 11	mSABc	2.14	2.09	2.01	1.86	15.77	13.77	2.00
N 3867 <sup>a</sup>	11 42 54.2	+19 40 40	SB0/a (edge)	2.32	2.35	2.31	2.27	14.93	12.62	2.31

Table 8. Annular- and Circular-aperture Photographic Photometry. -- Continued

Object	R.A. (1950)	Dec. (1950)	Type	2"-5"	5"-10"	7.5"-20"	10"-30"	U	R	U-R
N 3868	11 42 54.5	+19 43 20	SB0- pec	2.34	2.40	2.41	2.44	15.65	13.24	2.41
Anon 49	11 42 59.9	+19 41 39	E	2.04	1.99	2.03		16.83	14.77	2.06
N 3873	11 43 10.7	+20 03 06	E	2.34	2.32	2.28	2.24	14.57	12.28	2.29
N 3875	11 43 14.0	+20 02 42	S0pec(edge)	2.45	2.41	2.40	2.33	15.16	12.78	2.38
Anon 44	11 43 23.2	+20 04 51	S0+ pec:	2.13	2.03	2.03		16.90	14.79	2.11
Z97-143	11 43 30.8	+20 04 04	SB0/a	2.30	2.27	2.30		16.24	13.93	2.31
<u>A 2199</u>										
Anon 50	16 25 00.6	+39 41 50	SB0/a	2.06	2.15			17.10	15.02	2.08
Z224-27	16 25 20.5	+39 38 17	E	2.04	2.01	2.01	2.01	15.33	13.22	2.11
Anon 51	16 25 26.2	+39 43 48	S0 (edge)	1.90	1.87			17.61	15.71	1.90
Anon 52	16 25 46.8	+39 41 15	SAcd	1.70	1.36			17.76	16.15	1.61
Anon 53	16 25 49.4	+39 40 51	S0+	2.05	2.20			16.95	14.85	2.10
Anon 54	16 25 52.1	+39 35 36	S0 pec	1.91	1.79	1.70		17.07	15.26	1.81
N 6158	16 25 57.6	+39 29 35	E	2.28	2.13	2.10	2.15	14.97	12.80	2.17
Z224-34A	16 26 11.8	+39 22 07	E+	2.08	2.03	2.04	2.07	15.22	13.14	2.08
Anon 55	16 26 12.6	+39 23 28	E	2.14	2.07	2.09		16.18	14.07	2.11
Z224-34B	16 26 14.0	+39 21 45	SA0	2.13	2.07	1.90	1.73	15.71	13.79	1.92
Anon 56	16 26 15.6	+39 24 45	SB0+(R <sub>D</sub> )	2.15	2.20	2.19		16.51	14.33	2.18
Anon 57	16 26 15.8	+39 42 49	SB0+ pec	2.06	2.20	2.17		16.16	14.01	2.15
U 10404 <sup>a</sup>	16 26 29.2	+39 55 53	mSBab	2.31	1.99	1.99	1.96	15.01	12.99	2.02
Anon 58	16 26 40.5	+39 40 46	E	2.17	2.17	2.09	2.03	15.69	13.56	2.13
N 6166 <sup>a</sup>	16 26 55.6	+39 39 38	cD	2.26	2.35	2.37	2.33	14.15	11.83	2.32

Table 8. Annular- and Circular-aperture Photographic Photometry. -- Continued

Object	R.A. (1950)	Dec. (1950)	Type	2"-5"	5"-10"	7.5"-20"	10"-30"	U	R	U-R
Anon 59	16 26 56.3	+39 37 39	mSBd( $R_N$ )	2.10	2.13	2.04	1.91	15.96	13.90	2.06
Z224-40	16 27 01.4	+39 34 57	MSAb pec	2.26	2.33	2.19	2.10	15.35	13.16	2.19
Anon 60	16 27 02.0	+39 32 45	SA0+	2.23	2.29	2.24		16.50	14.25	2.25
Anon 61	16 27 03.1	+39 34 19	S0+ (edge)	2.03	2.16	2.20	2.28	16.14	13.97	2.17
Z224-44	16 27 07.7	+39 56 38	SABc	1.41	1.42	1.60	1.76	15.08	13.54	1.54
Z224-45	16 27 10.3	+39 40 08	SAC	1.11	1.08	1.23		15.74	14.60	1.14
Anon 62	16 27 14.7	+39 49 01	E	2.13	2.28			16.90	14.72	2.18
Anon 63	16 27 14.8	+39 25 39	SAB:	2.04	1.86	1.70	1.72	15.78	13.90	1.88
Anon 64	16 27 16.4	+39 54 42	S0-	1.93	2.04	2.00		15.95	13.96	1.99
Anon 65	16 27 17.1	+39 47 33	SAB0 pec	2.14	2.10			16.87	14.67	2.20
Anon 66	16 27 29.9	+39 46 45	SAB	1.99	1.75	1.70		15.57	13.73	1.84
Anon 67	16 27 33.5	+39 30 34	S0: (edge)	2.23	2.22	2.27		16.14	13.90	2.24
Anon 68	16 27 37.0	+39 32 13	mSB0/a( $R_N$ )	2.34	2.27	2.35	2.27	15.67	13.38	2.29
Anon 69	16 27 38.4	+39 55 43	S0: (edge)	2.10	1.98	2.11		16.15	14.05	2.10
Anon 70	16 27 40.6	+39 27 29	S0- pec	1.37	1.47			17.84	16.46	1.38
Anon 71	16 27 58.8	+39 51 21	S0 (edge)	2.04	2.09	2.03		17.10	15.02	2.08
Anon 72	16 28 05.5	+39 49 26	SABa	1.74	1.67	1.57	1.46	16.48	14.84	1.64
U 10420	16 28 08.7	+39 52 27	SBbc( $R_N$ )	2.16	2.09	1.48	1.22	14.78	13.31	1.47

a. Major axis > 1 arcminute.



The U and R magnitudes thus derived are fairly crude: as in photoelectric aperture photometry, the apertures usually include a large amount of sky, the photometry is taken to an arbitrary and changing surface brightness limit, the assumption of a constant sky value is questionable.

#### "Azimuthal" Photometry

For several galaxies, in particular those observed at 21-cm, a more controlled and accurate procedure was employed to find the magnitudes internal to the 26.5 magnitude/arcsec<sup>2</sup> B-band isophote. As in the photographic-and-photoelectric-photometry section of the observations chapter, accurate magnitudes in U and R were generated with the following procedure:

1. make a Fourier fit to the sky,
2. find the ellipticity and position angle of the outer isophotes of each galaxy,
3. using the information in 2., tabulate the average surface brightness values along azimuthal profiles until they merge into the sky,
4. employing the color-color relations, find the surface brightness in U and in R corresponding to  $B = 26.5$  magnitude/arcsec<sup>2</sup>,
5. from the azimuthal profiles find the brightness internal to the given isophote,

6. if B magnitudes are desired, convert from U and R to B using the color-color relation.

The color-color plots, described in the photoelectric photometry section of Chapter 2, were used for all instances in this study where U and R magnitudes were known and B magnitudes were needed, or where (U-B) or (B-R) was known and (U-R) was needed.

#### Photometry Comparisons and Error Trends

A comparison between the results of the "azimuthal" photometry, the circular photometry, and magnitudes given in the Uppsala General Catalog (Nilson 1973) are listed in Table 9. The  $m_{pg}$  from the UGC have been approximately corrected to B by the relation (Allen 1973)

$$B \approx m_{pg} + .11 \quad (8)$$

The UGC magnitudes systematically are higher than those of the present study. This trend is not entirely unexpected as it has also been observed by other researchers (Shostak 1978; Romanishin 1979, pers. comm.).

The discrepancies between magnitudes and colors determined in this investigation using two disparate methods can be almost entirely accounted for by the fixed apertures of the circular photometry; outer regions of NGC 494, UGC 1344, UGC 1350, UGC 6697, NGC 3860 and NGC 3861 lie outside

Table 9. Comparisons between Galaxy Magnitudes in Three Systems.

Name	Photometric Band	Circular-Aperture Magnitudes	"Azimuthal" Magnitudes	Magnitudes from UGC (Nilson 1973) [ $B=m_{pg} + .1$ ]
N 399	U	15.12	14.94	
	B		14.48	14.6
	R	12.82	12.67	
N 494	U	14.36	14.17	
	B		13.77	13.9
	R	12.25	12.05	
N 495	U	14.93	14.94	
	B		14.45	14.1
	R	12.66	12.66	
U 1344	U	14.10	14.05	
	B		13.66	14.1
	R	12.04	11.97	
U 1347	U	13.90	13.82	
	B		13.67	14.0
	R	12.42	12.29	
N 710	U	14.12	14.16	

Table 9.--Continued

Name	Photometric Band	Circular- Aperture Magnitudes	"Azimuthal" Magnitudes	Magnitudes from UGC (Nilson 1973) [B= m <sub>pg</sub> + .1]
U 1350	B		14.09	14.4
	R	12.80	12.81	
	U	14.91	14.62	
	B		14.24	14.6
U 6697	R	12.73	12.56	
	U	14.08	14.34	
	B		14.34	14.4
	R	13.07	13.14	
N 3860	U	14.65	14.57	
	B		14.24	14.6
	R	12.68	12.60	
	U	14.30	13.74	
N 3861	B		13.47	14.1
	R	12.34	11.91	
	U	14.83	14.78	
	B		14.44	15.5
U 10404	R	12.94	12.80	

the one arcmin aperture. In particular, in the case of NGC 3861, two actively-star-forming spiral arms lay beyond the largest circular aperture. The highly-inclined, vigorously-star-forming galaxy NGC 6697 also has disparate colors. A one-arcminute circular aperture does not contain all of the galaxy, and due to an inclination angle of approximately  $80^\circ$ , most of the aperture contains blank sky. For this galaxy in particular, the elliptical "aperture" of the azimuthal profiles increases signal to noise by decreasing the amount of extraneous "sky" measured.

One may well ask how severely the maximum one-arcmin diameters of the annular apertures will affect the results derived from colors of galaxies whose major axes extend beyond one arcmin. The color inaccuracies are most severe, as was seen for NGC 3861, for those galaxies with active star formation occurring in their arms. As will be seen presently, the smoothies are redder than the actively-star-forming, "clumpy" spirals of the same morphological type. This trend is actually decreased by the color inaccuracies due to too-small apertures. The clumpy spirals have more star formation than do the smooth-arm spirals and therefore are "reddened" more by not including outer regions in the surface photometry. Thus, inclusion of the outer regions would make the color differences between smoothies and normal spirals more pronounced.



## Color Comparisons between Smoothies and Normal Galaxies

To assess the differences in smooth-arm spiral colors from those of normal galaxies the following procedure was employed. All galaxies that were not smooth-arm spirals were binned as a function of morphological type. Galaxies were then removed from the sample if they were edge on, if they exhibited peculiarities, if their type was uncertain, or if they were too small, had too low surface brightness, or for some other reason did not have 7"5 - 20" aperture colors. E, E+, S0-, S0 and S0+ types had several (7 to 20) galaxies in each bin. The spirals, with fewer representatives, had adjacent bins combined as follows: S0/a and Sa, Sab and Sb, Sbc and Sc, Scd and Sd, Sm and I. The 5" - 10" aperture colors were averaged for each bin and 1 $\sigma$  error bars were assigned. The resultant color vs. morphological type is shown in Figure 4a. There appears a break in color at S0+; therefore the data are fitted with two different linear least-squares functions -- one from I to S0+ and one from S0+ to E. Figure 4b shows the least-squares fits from Figure 4a plotted with the 33 smooth-arm spirals. Triangles indicate good smoothies (type M), and crosses indicate fair ones (type m). A linear least-squares fit to these smoothy points follows the equation

$$(U-R) = .005(\text{type}) + 2.09 , \quad (9)$$

Figure 4. Color vs. Morphological Type for Non-smooth-arm Cluster Galaxies and for Smooth-arm Spirals.

- a. Average colors for each indicated type are shown with error bars. A least-squares fit to the data appears as a solid line.
- b. Color vs. type for the 33 smooth-arm spirals. The least-squares fit from (a) is again shown.

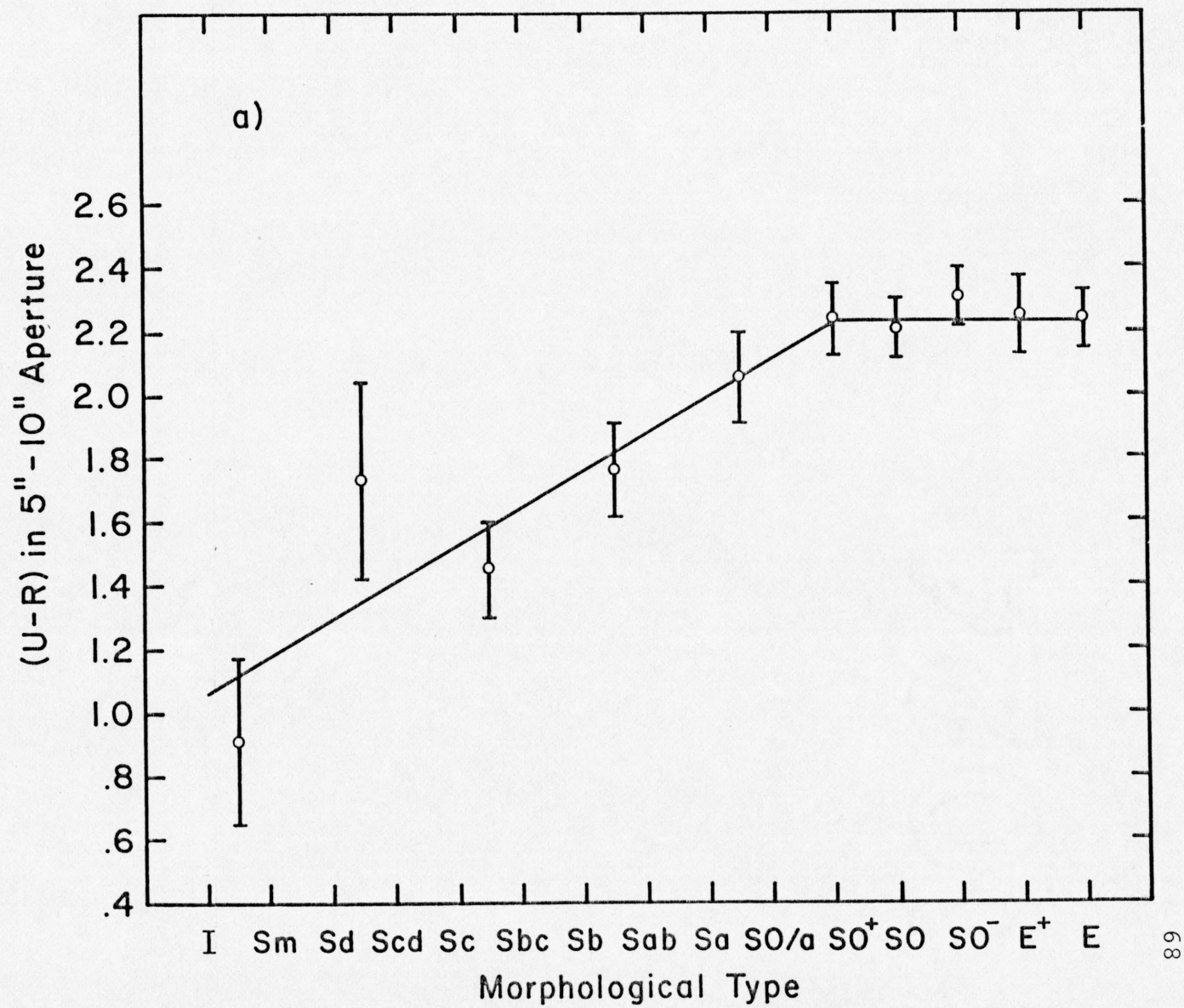


Figure 4. Color vs. Morphological Type

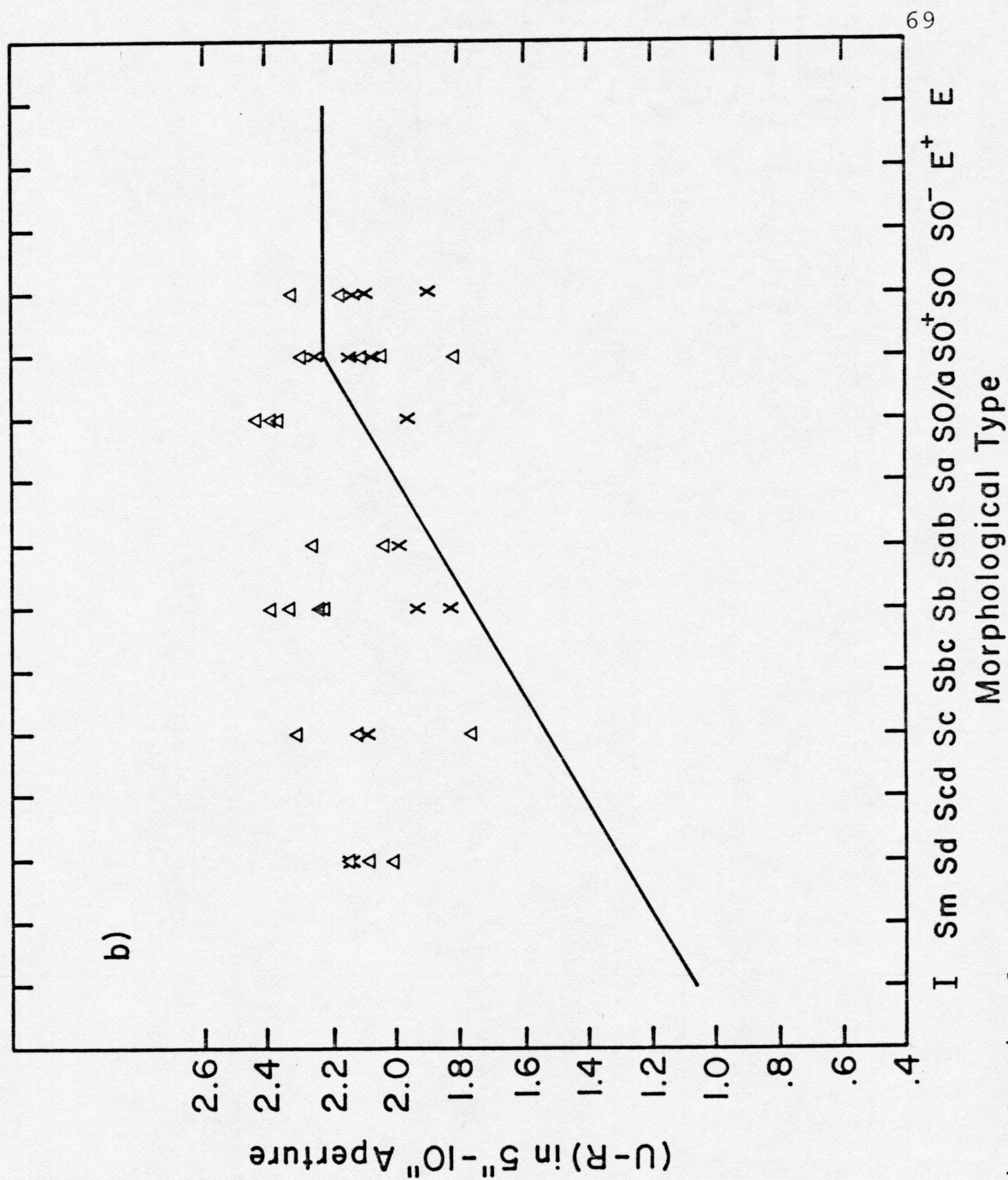


Figure 4. Continued.

where morphological types are assigned values as given in Table 10. The relation is consistent with  $(U-R) = 2.1$ . As can be seen from examination of Table 8 no trend exists for the smooth-arm spirals to be more luminous (or less luminous) than normal spirals of similar type. Thus the results shown in Figure 4 are not in actuality a consequence of higher luminosity. (Bluer galaxies tend to be less luminous.)

We wished to determine if the color separation for the later type galaxies was statistically significant. The normal galaxies whose colors had been used to derive Figure 4a were defined as two parent populations: one a spiral population including spirals from Sd to Sa, and the second an S0 population including S0/a, S0+ and S0. Mean values of 1.57 and 2.13, respectively, were derived for these two parent populations. The smooth-arm spirals were similarly divided and tested for significance of their deviation from the parent-population mean using a "Student's" t Test (student's t table from Langley [1971]). We find that the probability of the smooth-arm spirals classified as S0/a, S0+ and S0 having the same distribution of colors as the S0 parent population is greater than 10%. However the probability that the "spiral" smooth-arm spirals have the same distribution of colors as the spiral parent population is less than 0.2%. The statistics support the impression from

Table 10. Numerical Value Assignments  
for Morphological Types.

Type	Assigned Value
I	1
Sm	2
Sd	3
Scd	4
Sc	5
Sbc	6
Sb	7
Sab	8
Sa	9
S0/a	10
S0+	11
S0	12
S0-	13
E+	14
E	15

Figure 4 -- that the smooth-arm spirals later than Sa are significantly redder than the normal spirals.

#### Arm and Disk Surface Photometry

Thus far we have been dealing with integrated light from both the arm and disk regions. For several smooth-arm spirals, the arms were sufficiently separated and distinct that small-aperture photometry could be done separately in the arm (arm + disk) and interarm (disk) regions. The galaxies analyzed by this procedure were NGC 399, IC 1679, Z502-55, NGC 495, UGC 1344, UGC 1350, Anon 10, NGC 1264, NGC 1268, Z185-46, UGC 6393, UGC 10404, Z224-40 and Anon 68.

The arm colors, as measured in the several separate apertures, and the disk colors were averaged together. The averaged values were then subtracted from each other to give  $(U-R)_{\text{disk}} - (U-R)_{\text{arms}}$  for each of the above galaxies. The results are illustrated in Figure 5. The galaxies show results consistent with no color difference between arm and disk regions. The actively-star-forming spiral UGC 1347 in Abell 262 was measured using the same small-aperture-photometry procedure. For this galaxy the  $(U-R)_{\text{disk}} - (U-R)_{\text{arms}} = 0.46 \pm .15$ . Schweizer (1976) lists  $(U-R)_{\text{disk}} - (U-R)_{\text{arms}}$  for the following nearby galaxies:

$$\text{NGC 3031} = 0.83$$

$$\text{NGC 4254} = 0.86$$

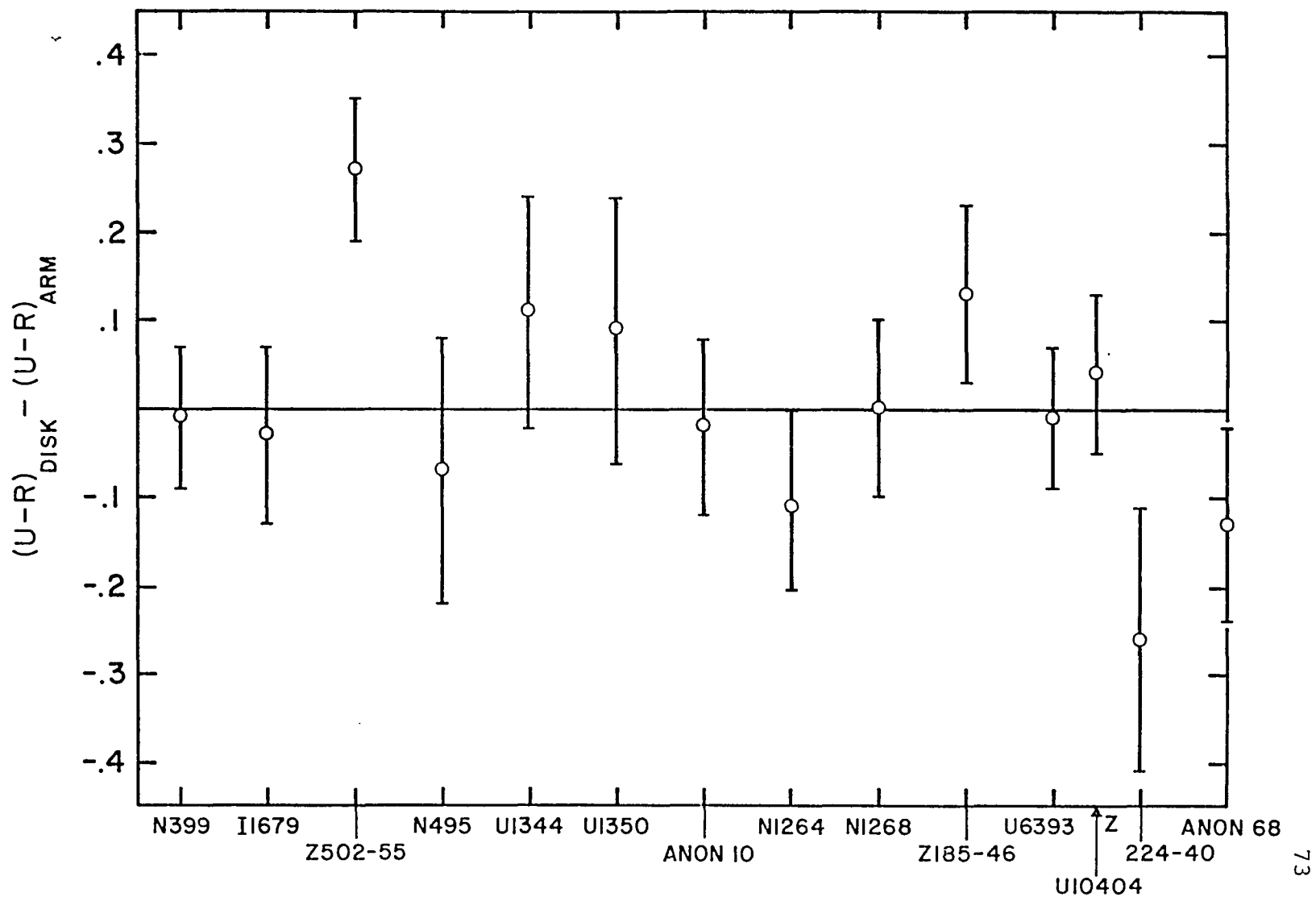


Figure 5. Values of  $(U-R)_{\text{disk}} - (U-R)_{\text{arm}}$  for Fourteen Smooth-arm Spirals.



$$\text{NGC 4321} = 0.78$$

$$\text{NGC 5457} = 0.85$$

Clearly the color differences between disks and arms are substantially smaller for smooth-arm spirals than for actively-star-forming spirals.

We also wished to look at the arm amplitudes of smooth-arm spirals. Toward this end the individual small apertures were plotted in surface brightness (magnitudes/arcsec<sup>2</sup>) vs. radius (corrected for inclination). For each galaxy four separate plots were made: arm and interarm regions in U and in R. Linear least-squares fits were made to the data in each plot. Eleven smooth-arm spirals exhibited well-defined linear relations. These galaxies are NGC 399, IC 1679, NGC 495, UGC 1344, UGC 1350, Anon 10, NGC 1264, NGC 1268, Z185-46, UGC 6393 and UGC 10404.

Four of the eleven smooth-arm galaxies show an increase in the arm amplitude with increasing radius. This trend was seen by Schweizer (1975) in normal spirals. A few -- IC 1679, UGC 1350 and NGC 1268 -- have essentially constant arm amplitudes. Three others -- NGC 495, UGC 6393 and UGC 10404 -- have decreasing arm amplitudes with increasing radius. It is not clear what this variation in arm amplitude with radius may imply, although, of those galaxies not exhibiting the behavior observed by Schweizer, all but NGC 1268 have bars.

A graph of the arm amplitude vs. integrated color was made to see if the arm amplitude changed as a function of galaxy color. In particular, if gas-depleted spirals evolve into S0s, then as the color reddens, indicating progressively longer times since the last epoch of star formation, the arms should die out. One might expect an exception to this trend in the epoch shortly after gas removal. The gas in a galaxy may act as a damping mechanism -- the density wave expends energy to condense the gas into stars. If the gas is removed, the amplitude of the stellar perturbation may increase for a time before turning over and beginning to die out. Speculations on the nature of the driving and damping mechanisms will be discussed in Chapter 4. The point to be made here is that the bluest smooth-arm spirals may not be expected to fit a systematic relation between arm amplitude and color.

To minimize the bulge contribution to disk light, the arm amplitudes were taken as the difference between the linear fits of arm and disk points at the largest radius at which both arm points and disk points still showed a clear linear relation (i.e., deviations  $>3\sigma$  from the linear fit, where  $\sigma$  is determined from the inner regions of the galaxy). Figure 6 plots the  $U_{\max}$  arm amplitude thus obtained against the (U-R) 5" - 10" annular aperture colors. For those galaxies with (U-R)  $>2.0$  a trend is indicated for redder

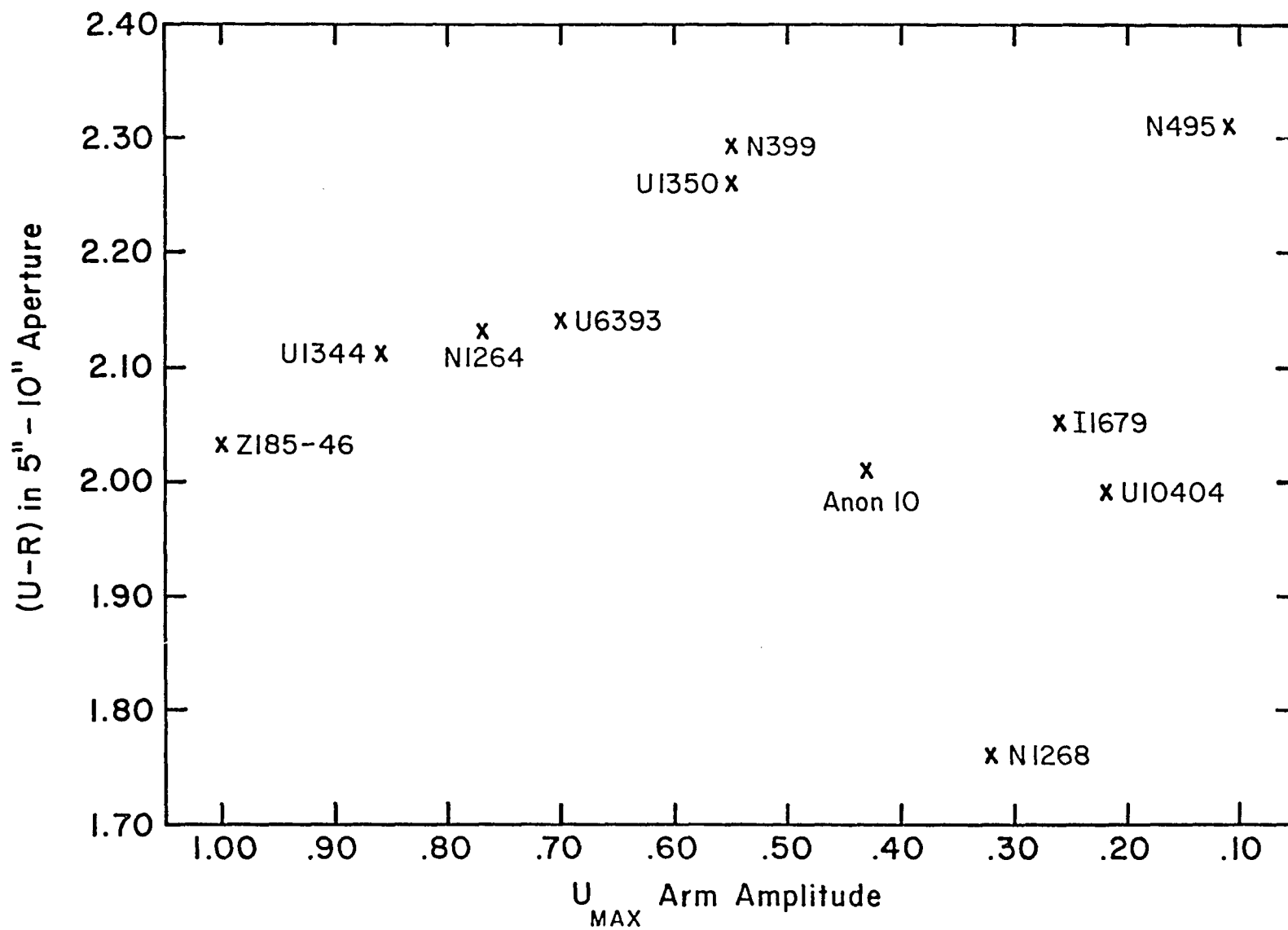


Figure 6. Plot of Color vs.  $U_{MAX}$  Arm Amplitude for Eleven Smooth-arm Spirals. -- The derivation of  $U_{max}$  arm amplitude is described in the text.

galaxies to have smaller arm amplitudes. There is a ~20% probability that this observed distribution would occur by chance. Four galaxies have moderately low arm amplitudes and relatively blue colors. In particular NGC 1268 is a clear exception to the trend discussed above. NGC 1268 (and possibly the other three deviant galaxies) may have had its gas removed more recently than the other seven, and has not yet reached its maximum arm amplitude.

As a density wave "dies out," due perhaps to removal of the driving mechanisms, then the arm strength will decrease. Arm strength can be considered as the area under the curve of brightness as a function of position for a cross section through the arm, the zero level being the underlying disk brightness. The arm amplitude, then is related to arm strength, but is not an absolute indicator.

A more subjective measure of arm strength, but one that takes into account the width of the arms and arm "definition" or the sharpness of the transition from inter-arm to arm, as well as their brightness amplitude, is to rank the galaxies by visual inspection. All the smooth-arm spirals were classified into one of the following three categories: (1) weak arms (incomplete arms or low-amplitude, poorly-defined arms), (2) moderate arms, (3) strong arms (good arm contrast, implying high amplitude, good definition, reasonable arm width). The ranking was

made from 4-m plates with all plates side-by-side for frequent intercomparisons. This procedure was used to maximize internal consistency. The ranking was repeated independently several days later. Those five galaxies whose classifications had changed were studied again and a final arm-strength rating was given. The final numbers of galaxies in each category were as follows: class 1 -- 9; class 2 -- 15; class 3 -- 9. Table 11 lists the galaxies and their colors in the 5" - 10" annular aperture according to their ranking. The average colors for each group are as follows:

class 3 --  $2.09 \pm .06$

class 2 --  $2.12 \pm .04$

class 1 --  $2.20 \pm .06$ .

The reddening of smooth-arm spirals with decreasing arm strength is at the  $1.3\sigma$  level. Although marginally significant, the trend is consistent throughout the three bins. One could argue that class 3 contains more late spirals and therefore that the above average colors actually are measuring morphological type rather than arm strength. However, the relation of morphological type vs. color essentially is a flat function for smooth-arm spirals. One would expect the convolution of the type with the arm-strength rankings to have little effect on the outcome.

Table 11. Arm-strength Rankings.

(3) Strong Arms		(2) Moderate Arms		(1) Weak Arms	
Name	Color	Name	Color	Name	Color
N 495	2.31	N 374	2.37	N 483	2.17
U 1344	2.11	N 399	2.29	N 503	2.06
U 1350	2.26	N 403	2.24	Z502-72	2.13
N 1268	1.76	I 1679	2.05	Anon 9	1.83
Anon 33	2.08	I 1682	1.96	Anon 34	2.32
N 3860	1.92	Z502-55	1.81	Anon 36	2.22
N 3864	2.09	Anon 2	1.89	Z97-101	2.43
U 10404	1.99	Anon 1	2.01	Z97-105	2.39
Z224-40	2.33	N1264	2.13	Anon 68	2.27
$\overline{(U-R)}=2.09+\underline{.06}$		Z185-46	2.03	$\overline{(U-R)}=2.20+\underline{.06}$	
		U 6393	2.14		
		Anon 41	2.10		
		I 2951	2.23		
		N 3857	2.39		
		Anon 59	2.13		
		$\overline{(U-R)}=2.12+\underline{.04}$			

### Comparisons between Morphological Classifications

The question may arise as to how sensitive the results in this section are to the accuracy of the morphological type assignments. Certainly, previous typings of smooth-arm spirals are suspect as many researchers base type in part on arm texture and color (see, for example, Nilson [1973] pp. III-IV). Thus smoothies would be typed systematically too early. Conversely it has been suggested that the types assigned herein may be too late. Separate comparisons were made between the morphological types of smooth-arm spirals and of other galaxies present both in this study and in the Uppsala General Catalog (Nilson 1973). Types were given numerical values of one unit each half type, as shown in Table 10. Each galaxy present in both studies is assigned a comparison index (CI) defined as

$$CI = (\text{type})_{\text{this study}} - (\text{type})_{\text{UGC}} . \quad (10)$$

A total of 56 galaxies were considered. The eleven smooth-arm spiral galaxies had an average  $CI = -1.00$ . The thirty other galaxies classified in both sources as S0- or earlier have an average  $CI = +0.18$ . If all the non-smoothy galaxies including E's are considered, the  $CI = -0.23$ . The change in CI with inclusion of early galaxies is due to coarseness of early classifications in the UGC. There are few instances of gradations between S0 and E. Thus

frequently what is referred to in the UGC as an E, Thompson classifies as E+ or S0-.

The low values for CI in the non-smooth sample would indicate that there are no systematic trends (except perhaps as noted above for late E galaxies) toward one classification source being later than another. The moderately high value of the comparison index for smooth-arm spirals would seem to indicate that previous studies tend to classify them too early due to factors noted above.

#### Disk-to-Bulge Ratios

The last of the measurements utilizing photographic surface photometry was the determination of disk-to-bulge (D/B) ratios. These ratios are important as indicators of the morphological type. (Morphological typing in this study was based primarily on D/B and pitch angle of the arms, or arm winding.) The quantitative deconvolution of the major-axis profile was complicated by (a) the large arm strengths, making disk determinations questionable at best, and (b) the presence of bars in many of the largest smooth-arm spirals. Inclusion of bar light in the major-axis scans can cause the bulge to appear larger, thereby giving erroneous values of the D/B ratios. Therefore, two methods were used to determine D/B: one quantitative; and one subjective, but better able to discount bar contributions.



A rigorous method of determining D/B is to deconvolve a disk system into an  $R^{1/4}$  bulge and an exponential disk. This method was found to be inefficacious due to the strength of the arms. Another quantitative method has been described by Burstein (in press, Paper II). It yields results consistent with the results obtained from deconvolution. In his " $R_4/R_x$ " method two radii are defined, the ratio of which are simply related to D/B. The "crossover" radius,  $R_x$ , is the radius where the B-luminosity contributions from the disk and from the bulge are equal. An exponential disk profile is drawn through the disk points and extrapolated to the center of the galaxy, as plotted in a surface brightness vs. radius graph.  $R_x$  is the radius at which the observed profile is 0.75 magnitudes brighter than the extrapolation. Burstein states that for systems with  $D/B > 1$ , the  $R_x$  thus measured is close to where the disk and the bulge are truly equal in surface brightness.

$R_4$  is defined as the radius at which a face-on S0 galaxy has a B luminosity 4 magnitudes fainter than the brightness at  $R_x$ . Corrections must be made for galaxy inclination and for photometric bands other than B. As the smooth-arm spirals have no active star formation, there is no need to correct for the galaxies not being S0s. Therefore, the quantity subtracted from the brightness at  $R_x$  to obtain  $R_4$  is  $[4 + 2.5 \log(b/a) + \Delta C]$ , where  $b/a$  is the

minor-to-major axis ratio, and  $\Delta C$  corrects passbands other than B for the color difference between bulge and disk. The  $R_4/R_x$  ratio thus derived can be converted to D/B using Burstein's (in press, Paper II) Figure 5.

Five smooth-arm spirals had major-axis scans which exhibited indications of the underlying disk luminosity, and had sufficiently large angular size that the bulge was resolved into at least 3 data points (semi-major axis of bulge  $\geq 6''$ ) before merging into the disk profile. Table 12 lists these galaxies, their assigned morphological type, minor-to-major axis ratio, color correction,  $R_4/R_x$ , D/B as derived from  $R_4/R_x$  [ $(D/B)_{4x}$ ], and D/B as estimated visually [ $(D/B)_{vis}$ , see below].

It is particularly difficult to obtain accurate quantitative D/B information from barred galaxies, lest the bar lie along the minor axis. This is seldom the case. For NGC 495 and UGC 1350 in particular the bar lies near the major axis. Therefore the D/B ratio also was measured by visual inspection. One can usually see an "edge" to the bulge where photographic density drops rapidly, and an "edge" to the disk where the disk brightness merges into sky background. The five smooth-arm spirals measured quantitatively also had D/B determined by this subjective visual method. The sky backgrounds of the four R plates viewed had densities from .34 to .47. Thus the exposures

Table 12. Disk-to-bulge Ratios for Five Smooth-arm Spirals. -- Headings are explained in text.

Name	Type	B/A	$\Delta C$	$R_x$	$R_4$	$R_4/R_x$	$(D/B)_{4x}$	$(D/B)_{vis}$
NGC495	SBC	.72	.11	3".1	25."	8.1	2.1	9.3
UGC1344	SBab	.70	.37	4.7	33.	7.0	1.3	6.4
UGC1350	SBC	.70	.05	1.9	31.	16.	5.9	9.6
NGC1268	SAC	.80	.12	1.5	32.	21.	9.0	12.5
UGC10404	SBab	.73	.20	3.2	35.	11.	3.3	7.0

recorded approximately equal brightness levels; the visual D/B measurements should not be greatly disparate due to differing locations of the bulge and disk density ranges on the respective characteristic curves.

Visual estimates of D/B for the three Sc's are larger than those for the two Sab's. The " $R_4/R_x$ " D/B for those galaxies without bars near the major axis give the same result: the one Sc D/B is larger than the two Sab D/B ratios. The  $R_4/R_x$  ratios determined here span the range of those found by Burstein (in press, Paper II) for S0s ( $R_4/R_x = 6$  to  $9$ ) and Sc's ( $R_4/R_x = 15$  to  $30$ ). We therefore conclude that our morphological designations are consistent with the disk-to-bulge ratios.

#### Other Optical Observations

##### The Search for Smooth-arm Spirals in the Field

Several dozen candidate smooth-arm spirals in the field or in small associations were noted on the Palomar Sky Survey. Nine of these galaxies were photographed to look for clumpiness at higher resolution (see Table 4). Poor weather precluded observing more. Of these nine, five were found to have distinct clumps of active star formation at the higher resolution. One galaxy, UGC 3723, remained indeterminate in that it showed hints of clumpiness, but it could be smooth. Two of the remaining three smooth

galaxies, Z285-13 and NGC 2859, are both SB0+. Thus, of eight "field" galaxies selected to be possible smooth-arm spirals, three galaxies, all S0 or S0+, are found to be smooth and five galaxies, all classical spirals, are found to not be smooth. This result is not surprising. Field S0 galaxies occur with less regularity than do cluster S0s (Biermann and Tinsley 1975), but they do occur nonetheless. This study will not try to suggest that all S0s, field and cluster, arise from stripped spirals. Other methods of gas depletion, including formation with little excess gas, must be causative of field and small-association S0s. To find field S0s shading into the continuum of smooth-arm spirals also is not unexpected.

The ninth galaxy of this sample, Z181-2, appears to be what the search was truly for -- a "field" smooth-arm spiral later than S0+. Nilson (1973) classifies the galaxy as an SBa. He also refers to it as a pair with UGC 4866.

Thus we find in the field that the ratio of actively-star-forming spirals to smooth-arm spirals ( $\text{Spi:Smo}$ ) is  $>5$ . The field galaxies studied here were selected due to their potential of being smooth-arm spirals. Those field galaxies obviously participating in current star formation were not photographed. Of those galaxies photographed as candidate smooth-arm spirals the  $\text{Spi:Smo}$  ratio is 5. The true  $\text{Spi:Smo}$  in the field must be

substantially larger. (It should be noted that this discussion does not include smooth-arm spirals classified traditionally as S0s.) The frequency of spirals in the field relative to S0s, Spi:S0, is 8 (Dressler, in press).

The ratio Spi:Smo for the clusters studied in this work, again not including "S0" smoothies, is as follows:

G383	--	3.0
Pisces	--	2.2
A 262	--	1.4
Perseus	--	0.6
A 1228	--	1.5
A 1367	--	1.9
A 2199	--	0.9.

Spi:S0 ratios, for the inner  $1^\circ$  of these clusters, were all  $<1.0$ .

It therefore appears that the rate of smooth-arm spirals in the field is substantially below that in clusters. The data also are not inconsistent with the field smooth-arm spirals being precursors of field S0 galaxies.

#### Spectroscopic Observations

The redshifts found (corrected to heliocentric) and emission lines seen have been given in Table 5. Those emission lines detected were all weak. All spectra showed G, H, and K lines -- many had Balmer lines in absorption.

### Neutral Hydrogen Results

Of the five smooth-arm spirals observed for neutral hydrogen, one galaxy -- UGC 1350 -- definitely was detected and one galaxy -- UGC 1344 -- possibly was detected at the  $\sim 2\sigma$  level. This possible detection has been treated in Table 6 as an upper limit, and the line parameters are listed with colons to indicate uncertainty. The smooth, baseline-subtracted spectra and the unsmoothed data with baseline indicated for UGC 1350 and UGC 1344 are shown in Figures 7 and 8, respectively. Figure 9 shows the spectrum toward NGC 495 as representative of the non-detections. The large spike at 4330 km/sec in Figure 9 and, to a lesser extent, in Figure 7 is due to interference at 1400.0 MHz.

A normal early-type spiral will have a neutral hydrogen mass-to-luminosity ratio of 0.1 to 0.4 in solar units (Balkowski 1973; Roberts 1975).  $M_{\text{HI}}/L_{\text{B}}$  will range up to 0.9 for late spirals. These data are for nearby field spirals or spirals in small associations. It has been found by Sullivan and Johnson (1978) that spiral galaxies in the Abell 1367 and Coma clusters are deficient in gas compared to those values listed above. Based on their detected  $M_{\text{HI}}/L_{\text{pg}}$  ratios and the rate of non-detections, they estimate that the  $M_{\text{HI}}/L_{\text{pg}}$  ratio for Abell 1367 is low by a factor of  $\sim 4$ , and that for Coma is low by a factor of  $\lesssim 10$ .



Figure 7. 21-cm Spectrum of UGC 1350.

- a. The data have been Hanning smoothed three times. The ordinate is flux in mJy. The abscissa is heliocentric velocity in  $\text{km s}^{-1}$ . The arrow indicates center of the radio neutral hydrogen line.
- b. Unsmoothed spectrum of UGC 1350. The unsubtracted baseline is shown as a solid line. Axes are as in (a).

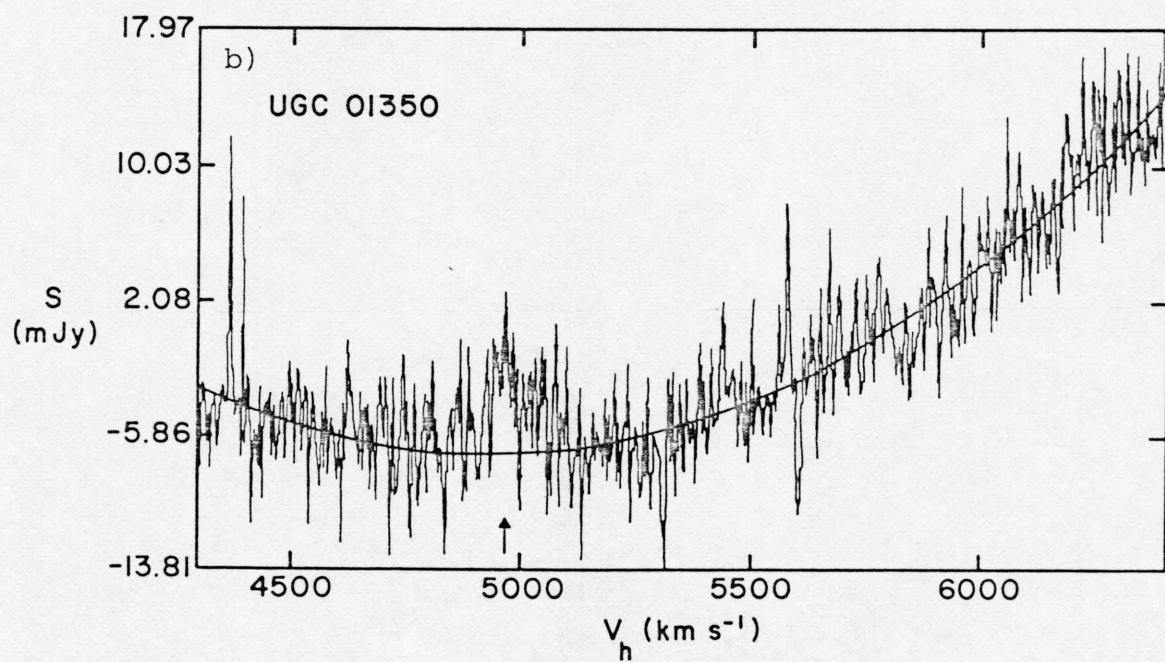
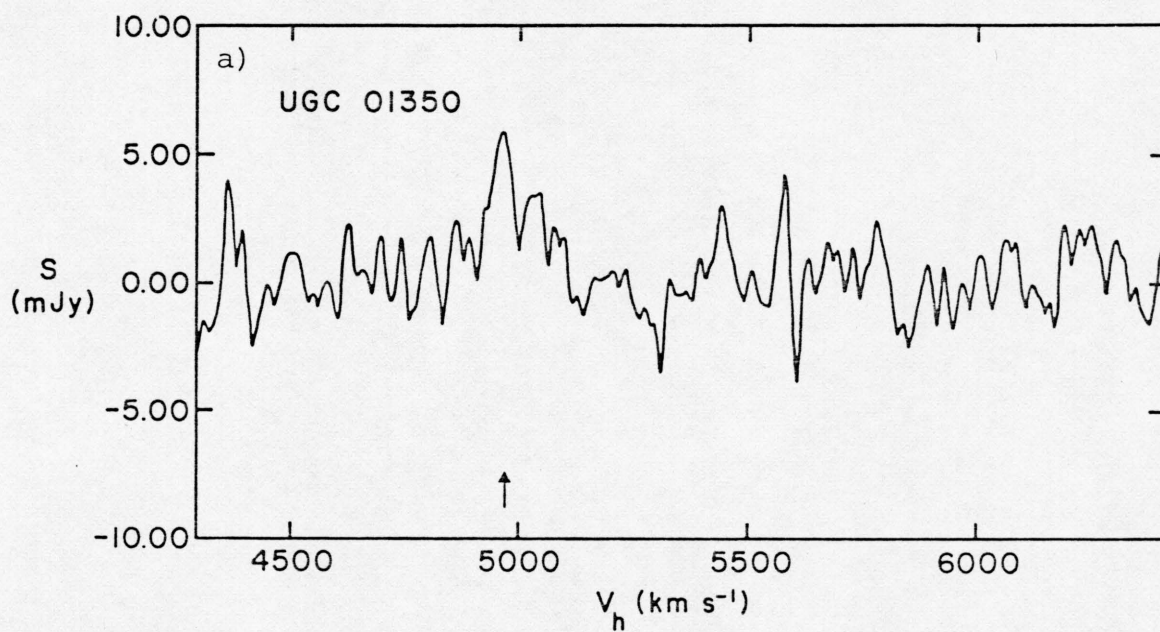


Figure 7. 21-cm Spectrum of UGC 1350.

Figure 8. 21-cm Spectrum of UGC 1344.  
a. Same as Figure 7a; for UGC 1344.  
b. Same as Figure 7b; for UGC 1344.

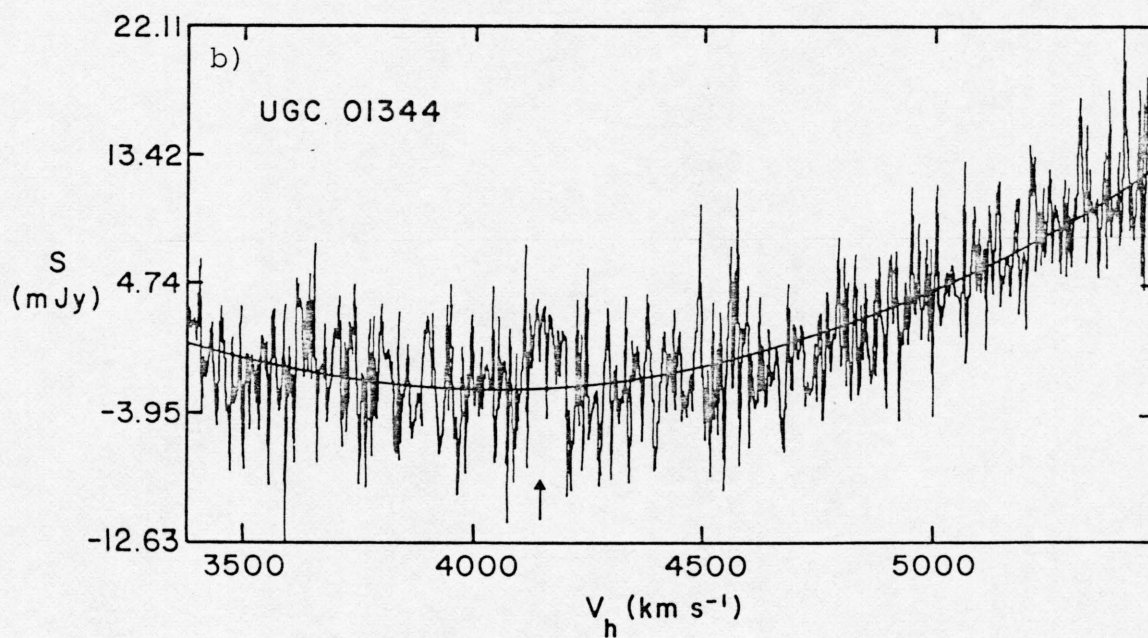
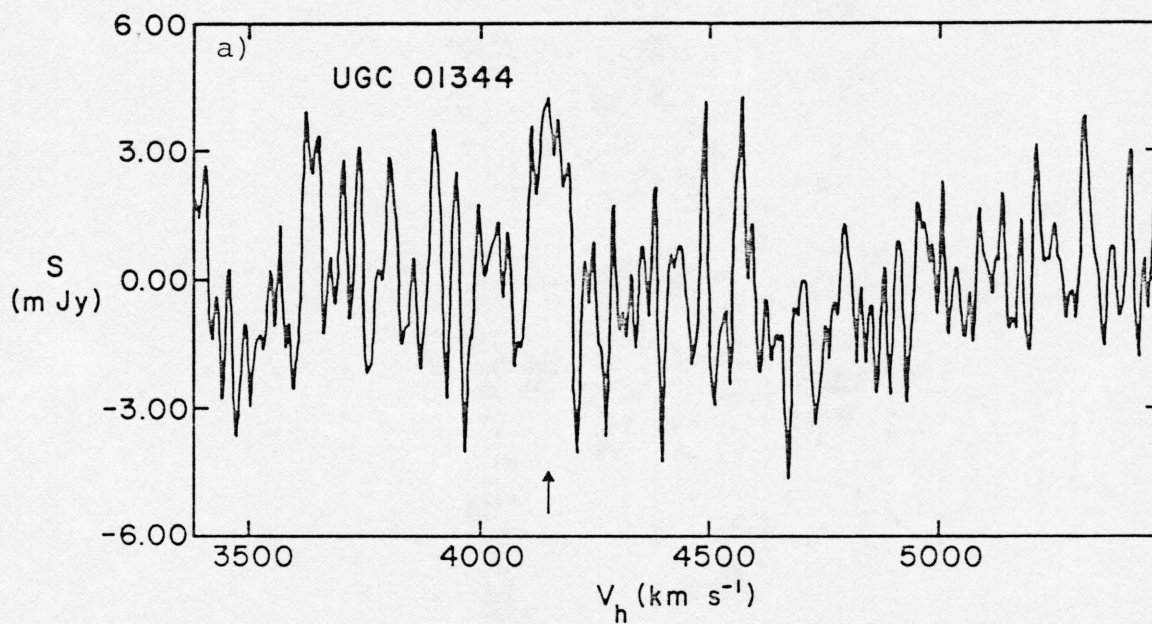


Figure 8. 21-cm Spectrum of UGC 1344.

Figure 9. 21-cm Spectrum toward NGC 495.  
a. Axes as in Figure 7a. The optical redshift  
is indicated by an arrow.  
b. Same as Figure 7b; for NGC 495.

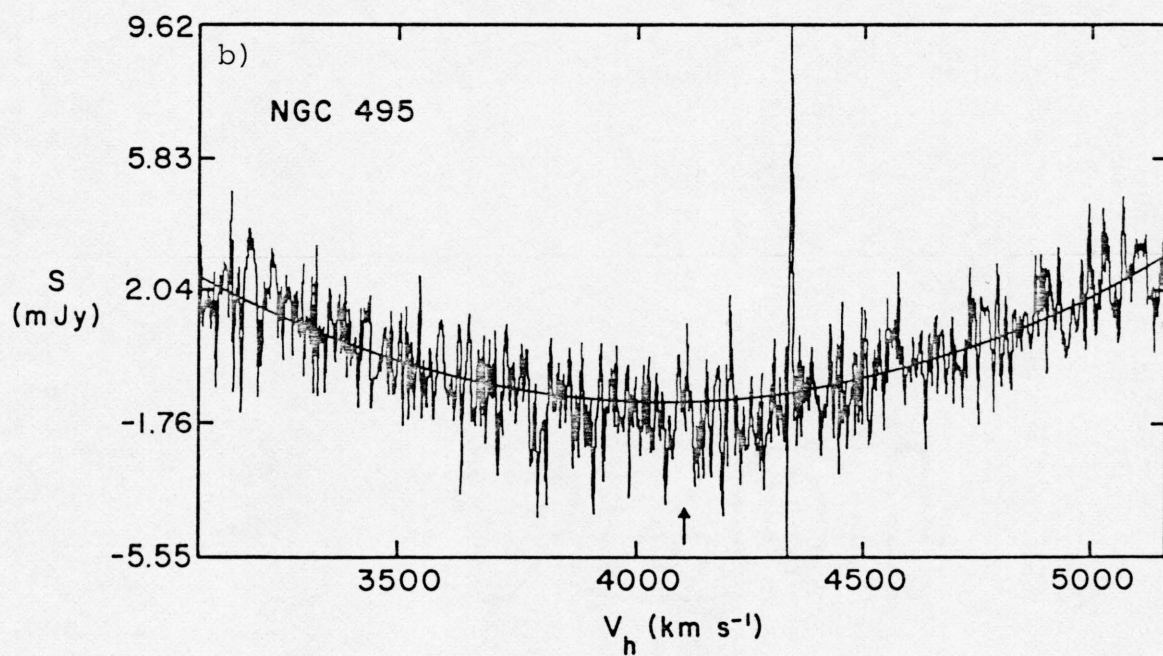
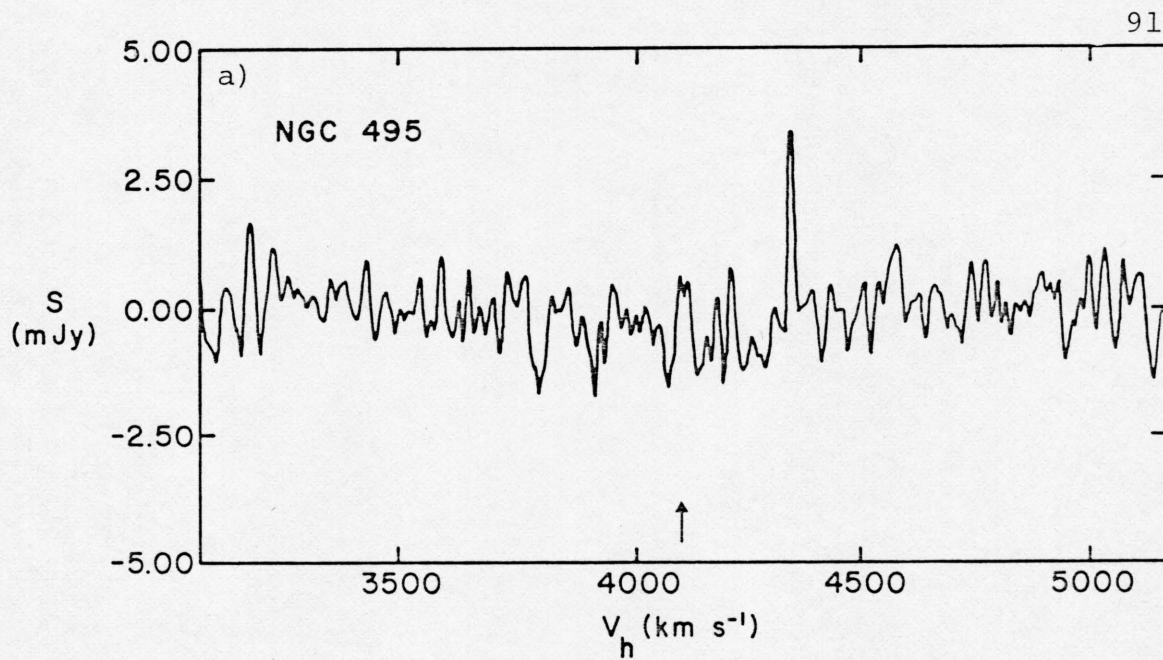


Figure 9. 21-cm Spectrum toward NGC 495.



It is found in this study that part of the extreme deficiency in Coma may be due to the inclusion of smooth-arm spirals in the observed sample. The Sullivan and Johnson Abell 1367 sample is essentially free of smooth-arm spirals. Two non-smooth spirals were detected in Abell 1367 in the observations made for the present study. NGC 3861 is found to be deficient by a factor of 4. UGC 6697 has an extended wing which passed beyond the edge of the spectrum; no deficiency factor has been estimated. The non-smooth galaxies UGC 1347 and NGC 710 in Abell 262 are deficient, respectively, by factors of 2.25 and  $>1.8$ .<sup>3</sup>

The smooth-arm spirals, on the other hand, are deficient by much greater factors. It is found that smoothies are low by the following factors:

NGC 399  $> 1$ .

NGC 495  $> 9$ .

UGC 1344  $\geq 8$ .

UGC 1350 = 10.

NGC 3860  $> 3$ .

The deficiency factors are quite sensitive to Hubble classification. Although the galaxies were typed using 4-m

---

<sup>3</sup>It must be noted that NGC 710 does not have a published redshift known to the author, nor does the author have a spectrum of the galaxy. It is possible, therefore, that the redshifted H I line of NGC 710 lies outside the observed spectrum.



plate material in 3 colors, the types could be disputed up to typically half a division (de Vaucouleurs 1959) due to the subjectivity of such morphological typing. The above results thus could be altered by roughly a factor of 2. Even then the smooth-arm spirals can be seen to be deficient in neutral hydrogen, typically even more deficient than rich-cluster, non-smooth spirals.

## CHAPTER 4

### DISCUSSION

In the Introduction a scenario was proposed for a spiral galaxy that had its gas removed in a single stripping event -- no doubt a simplistic assumption, but one that shall be adopted in the following discussion. Briefly, the scenario proceeded as follows: removal of gas, gradual dying of disk density wave, emergence of S0 galaxy. This procedure produces several observational ramifications.

If the stripping event removes most or all interstellar gas such that the spiral galaxy has little or no material from which stars may form, the galaxy's luminosity will come predominantly from progressively older stars -- thus galaxy colors will become progressively redder. As a consequence, smooth-arm spirals should be redder than actively-star-forming spirals of the same morphological type. As the disk density wave becomes weaker, the galaxy gradually assumes the appearance of an S0. Therefore some of the smooth-arm spirals classified traditionally as S0 should be somewhat bluer than average as they have undergone star formation more recently than most. There also should be a rough correlation between the strength of the

arms and the color of the non-nuclear regions, as both parameters are changing with time since the gas-removal event (GRE). Thus galaxies with strong, prominent arms should, on the average, have bluer colors than those with weak, vestigial arms.

We have seen in the previous chapters that all above criteria are met. Figure 4b demonstrates both the anomalously red colors for morphological type of the later smooth-arm spirals, and the essentially normal colors of the S0/a - S0 smoothies. We also have seen in Table 11 and in Figure 6 that bluer smooth-arm spirals tend to have larger arm strengths and arm amplitudes than do the redder galaxies in the sample. The arm-strength/color correlation is weak.

Constraints can be placed on the time since the GRE. The bluest smooth-arm spiral studied as a (U-R) color of 1.76; the reddest, 2.43. By using Table 1 of Biermann and Tinsley (1975) and equation 5 of the present work, we find that the times since the GRE range from a few  $\times 10^8$  years to  $\sim 6 \times 10^9$  years, with most falling around 1 to  $3 \times 10^9$  years.

The neutral hydrogen data also can provide a time constraint. The detected galaxy, UGC 1350, in particular can be employed toward determining a minimum time since the GRE. Biermann and Tinsley (1975) set two extreme cases for

the rate of star formation prior to the GRE. Star formation is zero after the GRE. The actual rate would lie between the two cases. The first case assumes a single burst of star formation at the time the galaxy was formed. The ratio of the gas mass injected into the interstellar medium from dying stars to B luminosity, assuming all interstellar gas was lost at the time,  $t_s$ , of the GRE, can be approximated by

$$M_{\text{HI}}/L_B \approx 1.7[1 - (t_s/t_o)^{0.11}] , \quad (11)$$

where  $t_o$  is the present time. The other extreme, that of continuous star formation up to the GRE, yields the following equation:

$$\frac{M_{\text{HI}}}{L_B} = 0.2 \frac{1 - (t_s/t_o)^{1.1} - [1 - (t_s/t_o)]^{1.1}}{1 - [1 - (t_s/t_o)]^{0.14}} \quad (12)$$

UGC 1350 has  $M_{\text{HI}}/L_B = .036$ . Assuming the age of the galaxy is  $11 \times 10^9$  years, we find that the minimum time since the GRE,  $t_{\text{GRE}}$ , lies between  $1.5 - 2.0 \times 10^9$  years for this galaxy. This value is indeed a minimum time as gas mass is frequently severely underabundant in red galaxies such as Es and S0s. It has been presumed that some internal sweeping mechanism, such as galactic winds from supernovae or flare stars, may remove much interstellar gas in low-gas systems (e.g., Coleman and Worden 1977; Mathews and Baker 1971; Faber and Gallagher 1976). This minimum

$t_{\text{GRE}}$  for UGC 1350 is entirely consistent with the  $t_{\text{GRE}}$  derived from color, which is roughly  $0.8$  to  $1.8 \times 10^9$  years. Apparently little gas accumulated since the GRE has been lost from this system. As mentioned in Chapter 3, though, UGC 1350 is deficient in neutral hydrogen as compared to an unstripped, actively-star-forming, field spiral of the same morphological type, by a factor of 10.

Those smooth-arm spirals observed in 21-cm but not detected can yield little information on  $t_{\text{GRE}}$  as they provide only an upper limit to a minimum. UGC 1344, however, was possibly detected. Treating it as a detection we find from the HI mass

$$t_{\text{GRE}} \geq 0.6 - 0.9 \times 10^9 \text{ years}$$

and from the color evolution

$$t_{\text{GRE}} = 0.9 - 1.7 \times 10^9 \text{ years.}$$

The calculations indicate that some subsequent gas loss has probably occurred in UGC 1344.

The results presented in this work are consistent with and supportive of the hypothesis that smooth-arm spirals are galaxies in transition between actively-star-forming spirals and S0 galaxies, with the transition initiated by removal of the interstellar gas. The nature of this gas-removal mechanism appears to be of a sort that



occurs predominantly in clusters of galaxies. The two mechanisms suggested most frequently for gas removal in clusters are galaxy collisions and ram-pressure stripping. If galaxy collisions are the predominant method for gas removal, then there should be a correlation between cluster richness and ratio of spirals to smoothies (Spi:Smo). If ram-pressure stripping predominates, then there must be a hot intracluster medium. Intracluster media have been identified in a number of clusters by x-ray observations (e.g., observations -- Cooke et al. 1978; McKee et al. 1979, in prep.; interpretations -- Serlemitsos et al. 1977; de Young 1978). Therefore, stripping should imply a correlation between the presence of detected intracluster x-ray emission and smoothies, with the stronger x-ray emitters associated with a lower Spi:Smo. Figure 10 presents these two graphs for 5 Abell clusters (Pisces and G383 are not Abell clusters). The x-ray data, except for Perseus, were kindly provided in advance of publication by McKee et al. 1979 in prep.). The Perseus x-ray luminosity is taken from Cooke et al. (1978). The Spi:Smo ratio was calculated in the cluster cores (inner  $1^\circ$ ) and does not include "S0" smoothies. Table 13 lists the total number of galaxies (Spi + Smo) counted in each cluster. Figure 10a indicates a very weak trend for the Abell richness class to be inversely correlated with the ratio of clumpy spirals to

Figure 10. X-ray Luminosity and Abell Richness Class vs. Spi:Smo Ratio for Five Abell Clusters Containing Smooth-arm Spirals.

- a. Abell (1958) richness class vs. Spi:Smo.
- b. The log of the x-ray luminosity vs. Spi:Smo for sample as in (a).



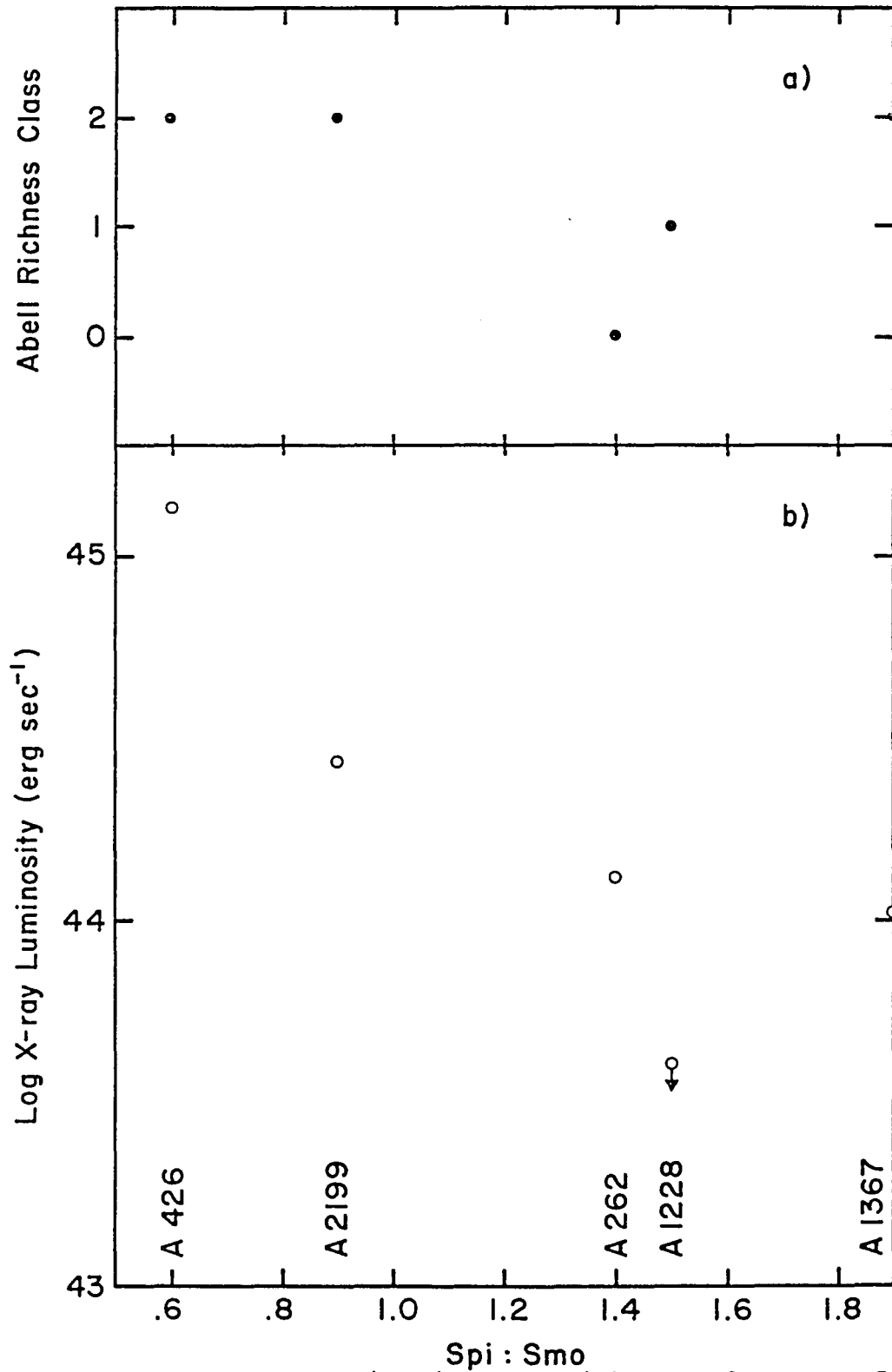


Figure 10. X-ray Luminosity and Richness Class vs.  $S_{pi}:S_{mo}$ .

Table 13. Total Galaxy Counts and Spi:Smo Ratio.

	Spi+Smo	Spi:Smo
G383	12	3.0
Pisces	13	2.2
A262	12	1.4
Perseus	11	0.6
A 1228	13	1.5
A1367	20	1.9
A2199	13	0.9

smooth spirals. It is well known that the ratio of the number of spirals to all galaxies, or spirals to S0s, decreases with increasing central cluster density, and that there is a correlation between central density and x-ray luminosity (Bahcall 1977a, 1977b). The Spi:Smo ratio, however, appears to be only weakly related to the richness class. On the other hand the Spi:Smo ratio exhibits a good inverse correlation with the cluster x-ray luminosity as shown in Figure 10b. Thus ram-pressure stripping would seem to be the dominant stripping mechanism.

It has been suggested that smooth-arm spirals are not stripped spirals, but rather are all early Sa galaxies (Sandage 1979, pers. comm.). In this scenario the gas deficiency is explained without invoking stripping; most H I measurements of early Sa types in the field have resulted in non-detections. If smooth-arm spirals are a subset of the Sa class, then the Spi:Smo ratio determined above should be greater than the ratio of all Sa galaxies to spiral galaxies. As discussed earlier, the Spi:Smo includes only smoothies that are classed as spirals. All clumpy spirals are counted. Thus Spi:Smo should be conservatively large. We have seen Spi:Smo equals 0.6 to 1.9.

Kraan-Kortweg and Tammann (in press, hereafter KT) have compiled a distance-limited sample of nearby galaxies ( $\leq 10$  Mpc). From their data we tabulated the spirals

classed as Sc, Sbc and Sb, and the galaxies classed as Sa and S0/a. As we are not including the Sab, Scd or Sc spirals, and we are including S0/a's, the Spi:Sa ratio thus derived from KT should be conservatively small. This ratio of  $(Sc+Sbc+Sb):(Sa+S0/a)$  equals 4.1.

As intrinsically fainter galaxies tend to be later in morphological type, it may be argued that our cluster-galaxy counts discriminate against fainter, later galaxies with small absolute magnitudes. Therefore, we measured the radii of the smallest-angular-diameter galaxy in each cluster that was included in the cluster galaxy counts. The radii were converted to crude absolute magnitudes using a relation given by Peterson, Strom and Strom (1979) derived for the Virgo Cluster. These limiting absolute magnitudes for each cluster are given in Table 14. The brightest absolute-magnitude limit is  $\sim 17.9$ .  $(Sc+Sbc+Sb):(Sa+S0/a)$  was again tabulated from KT, this time admitting only galaxies with  $M_B < -18.0$ .  $(Sc+Sbc+Sb):(Sa+S0/a)$  is thus reduced to 3.8. The data clearly indicate that smooth-arm spirals are not an Sa population. The wide range of disk-to-bulge ratios also indicates a greater diversity of morphological types. Gas removal by some mechanism again appears to have influenced the smooth-arm spirals.

After stripping of an actively-star-forming spiral, once again making the assumption that stripping is a single,

Table 14. Limiting Absolute Magnitudes for Galaxies Considered in Cluster Galaxy Counts. -- To conform with Peterson, Strom and Strom (1979), in this table  $H_0 = 50 \text{ km sec}^{-1} \text{ Mpc}^{-1}$ . The radius in kpc of the smallest galaxy included is given in r column;  $M_B$  is the absolute B magnitude.

	r (kpc)	$M_B$
G 383	6.3	-17.7
Pisces	3.4	-16.0
A 262	4.8	-17.0
Perseus	6.7	-17.9
A 2199	4.9	-17.1
A 1367	6.0	-17.6
A 2199	5.5	-17.4

short-duration event, a smooth-arm spiral presumably would be recognizable in  $\sim 10^7$  years, or the time scale for O and B stars to die. Color arguments indicate that smooth-arm spirals can last at least  $4 - 6 \times 10^9$  years before completely losing vestigial arms.

The gas in a spiral galaxy damps the density wave as the perturbation loses energy from gas compression and star formation (Toomre 1977). Presumably, therefore, the energy in the wave and the perturbation of the stellar component (and thus stellar arm strength) would initially rise after stripping. Indeed we see smooth-arm spirals where the peak stellar density enhancement in the arms relative to the disk is  $\sim 65\%$  (see Figure 7) -- roughly twice the stellar-population enhancement of "normal" spirals.

The mechanisms by which density waves are generated and sustained are not known, although several methods have been proposed (Wielen 1974). Lin (1970, 1971) has suggested that density waves may be caused by Jeans instabilities in the H I gas in the outer regions of the galaxy. The removal of this gas in stripping would thereby remove a possible wave driving mechanism. Another maintenance source that would cease after stripping is energy input from young stars (Biermann 1973). That the wave does not damp out in  $< 10^9$  years would suggest that either (a) with the interior gas, a major damping mechanism, removed the

density wave can continue even without energy input for  $\sim 5 - 6 \times 10^9$  years, or (b) more than the above mechanisms are at work driving the density wave; with some of the energy sources removed the others, such as perturbations introduced by interactions with other galaxies in a cluster, can prolong the wave's lifetime for a finite period but cannot sustain the wave indefinitely.



## REFERENCES

- Abell, G. O. 1958, Ap. J. Suppl., 3, 211.
- Allen, C. W. 1973, Astrophysical Quantities (London: Athlone Press).
- Bahcall, N. A. 1977a, Ap. J. (Letters), 217, L77.
- \_\_\_\_\_. 1977b, Ap. J. (Letters), 218, L93.
- Balkowski, C. 1973, Astr. and Ap., 29, 43.
- Biermann, P. 1973, Astr. and Ap., 22, 407.
- \_\_\_\_\_ and B. M. Tinsley. 1975, Astr. and Ap., 41, 441.
- Bridle, A. H., M. M. Davis, E. B. Fomalont and J. Lequeux. 1972, A. J., 77, 405.
- Burstein, D. In press, Ap. J. (Paper II).
- \_\_\_\_\_. In press, Ap. J. (Paper III).
- Butcher, H. and A. Oemler, Jr. 1978a, Ap. J., 219, 18.
- \_\_\_\_\_. 1978b, Ap. J., 226, 559.
- Chincarini, G. and H. J. Rood. 1971, Ap. J., 168, 321.
- Coleman, G. D. and S. P. Worden. 1977, Ap. J., 218, 792.
- Cooke, B. A., M. J. Ricketts, T. Maccacaro, J. P. Pye, M. Elvis, M. G. Walson, R. E. Griffiths, K. A. Pounds, I. McHardy, D. Maccagni, F. D. Steward, C. G. Page and M. J. L. Turner. 1978, M.N.R.A.S., 182, 489.
- de Vaucouleurs, G. 1959, in Handbuch der Physik, vol. 53, ed. S. Flügge (Berlin: Springer-Verlag) p. 275.
- \_\_\_\_\_ and A. de Vaucouleurs. 1976, Second Reference Catalog of Bright Galaxies (Austin: University of Texas Press).

- de Young, D. S. 1978, Ap. J., 223, 47.
- Dressler, A. In press, Ap. J., "Galaxy Morphology in Rich Clusters: Implications for the Formation and Evolution of Galaxies."
- Eastman Kodak Company. 1973, "Kodak Plates and Films for Scientific Photography."
- Faber, S. M. and J. S. Gallagher. 1976, Ap. J., 204, 365.
- Forman, W., J. Schwarz, W. Liller and A. C. Fabian. In press, Ap. J. (Letters), "X-ray Observations of Galaxies in the Virgo Cluster."
- Gisler, G. R. 1979, Ap. J., 228, 385.
- \_\_\_\_\_. 1979, in preparation, NRAO Charlottesville, VA, "Emission Lines in Elliptical Galaxies."
- Goad, L. E. 1975, Ph. D. thesis, Harvard University.
- Gudehus, D. H. 1976, Ap. J., 208, 267.
- Gunn, J. E. and J. R. Gott III. 1972, Ap. J., 176, 1.
- Hubble, E. 1926, Ap. J., 64, 321.
- \_\_\_\_\_. 1936, The Realm of the Nebulae (New Haven, Conn.: Yale University Press).
- Humason, M. L., N. U. Mayall and A. R. Sandage. 1956, A. J., 61, 97.
- Jensen, E. B. 1977, Ph. D. dissertation, Univ. of Arizona.
- Johnson, H. L. 1963, in Stars and Stellar Systems, III. Basic Astronomical Data, ed. K. Aa. Strand (Chicago: University of Chicago Press) p. 204.
- \_\_\_\_\_. 1965, Ap. J., 141, 923.
- Johnson, H. L. and W. W. Morgan. 1951, Ap. J., 114, 522.
- Knapp, G. R., J. S. Gallagher, S. M. Faber and B. Balick. 1977, A. J., 82, 106.
- Knapp, G. R., F. J. Kerr and B. A. Williams. 1978, Ap. J., 222, 800.

- Kraan-Korteweg, R. C. and G. A. Tammann. In press, Astronomische Nachrichten, Germany, "A Catalog of Galaxies Within 10 Mpc."
- Kron, G. E. and J. L. Smith. 1951, Ap. J., 113, 324.
- Landolt, A. U. 1973, A. J., 78, 959.
- Langley, R. 1971, Practical Statistics Simply Explained (New York: Dover Publications, Inc.).
- Lea, S. M. and D. S. de Young. 1976, Ap. J., 210, 647.
- Lin, C. C. 1970, in I. A. U. Symp. No. 38 (Dordrecht, Holland: D. Reidel Publishing Co.) p. 377.
- \_\_\_\_\_. 1971, in Highlights of Astronomy, vol. 2, ed. C. de Jager (Dordrecht, Holland: D. Reidel Publishing Co.) p. 88.
- Mathews, W. G. and J. C. Baker. 1971, Ap. J., 170, 241.
- McKee, J. C., R. F. Mushotsky, S. H. Pravdo, F. E. Marshall, E. A. Boldt, S. S. Holt and P. J. Serlemitsos. 1979, in prep., NASA/Goddard Green Belt, MD, "X-ray Emission from Abell Clusters Not Near Perseus."
- Melnick, J. and W. L. W. Sargent. 1977, Ap. J., 215, 401.
- Moffet, T. J. and T. G. Barnes. 1979, A. J., 84, 627.
- Moss, C. and R. J. Dickens. 1977, M.N.R.A.S., 178, 701.
- Nilson, P. 1973, Uppsala General Catalog of Galaxies (Uppsala: Uppsala Offset Center).
- Pence, W. 1976, Ap. J., 203, 39.
- Peterson, B. M., S. E. Strom and K. M. Strom. 1979, A. J., 84, 735.
- Roberts, M. S. 1969, A. J., 75, 859.
- \_\_\_\_\_. 1975, in Stars and Stellar Systems, IX. Galaxies and the Universe, eds. A. Sandage, M. Sandage and J. Kristian (Chicago: Univ. of Chicago), Chap. 9.
- \_\_\_\_\_. 1978, A. J., 83, 1026.

- Romanishin, W. 1979, in prep., Ph. D. dissertation,  
University of Arizona, Department of Astronomy.
- \_\_\_\_\_. 1979, pers, comm., postdoctoral fellow, UCLA.
- Sandage, A. 1961, The Hubble Atlas of Galaxies (Washington, D. C.: Carnegie Institution of Washington).
- \_\_\_\_\_. 1973, Ap. J., 183, 711.
- \_\_\_\_\_. 1979, pers, comm., scientific staff, Hale Obs.
- Schild, R. and J. B. Oke. 1971, Ap. J., 169, 209.
- Schweizer, F. 1975, in La Dynamique des Galaxies Spirales,  
ed. L. Weliachew (Paris: Centre National de la  
Recherche Scientifique), p. 337.
- \_\_\_\_\_. 1976, Ap. J. Suppl., 31, 313.
- Serlemitsos, P. J., B. W. Smith, E. A. Boldt, S. S. Holt  
and J. H. Swank. 1977, Ap. J. (Letters), 211, L63.
- Shostak, G. S. 1978, Astr. and Ap., 68, 231.
- Spitzer, L. Jr. and W. Baade. 1951, Ap. J., 113, 413.
- Strom, S. E. In press, Ap. J., "Toward a Physical Under-  
standing of the Hubble Sequence."
- \_\_\_\_\_, E. B. Jensen and K. M. Strom. 1976, Ap. J.  
(Letters), 206, L11.
- Sullivan, W. T. III and P. E. Johnson. 1978, Ap. J., 225,  
751.
- Sullivan, W. T. III, R. A. Schommer and G. D. Bothun. 1979,  
pers. comm., University of Washington.
- Thompson, L. A. 1978, pers. comm., asst. prof., Univ. Hawaii.
- Tifft, W. G. 1978, Ap. J., 222, 54.
- \_\_\_\_\_, K. A. Hilsman and L. C. Corrado. 1975, Ap. J.,  
199, 16.
- Toomre, A. 1977, Ann. Rev. A. Ap., 15, 437.
- van den Bergh, S. 1976, Ap. J., 206, 883.

- van den Bergh, S. In press, Phil. Trans. Royal Soc. London,  
"The Classification of Evolving Galaxies."
- Wakamatsu, K. 1976, Publ. Astron. Soc. Japan, 28, 397.
- Wells, D. 1975, KPNO and CTIO Quarterly Bull., July-Sept.,  
p. 12.
- Whitford, A. E. 1971, Ap. J., 169, 215.
- Wielen, R. 1974, Publ. A. S. P., 86, 341.
- Wilkerson, M. S., S. E. Strom and K. M. Strom. 1977, Bull.  
Amer. Astr. Soc., 9, 649.